

Sample size and power calculations for causal inference in observational studies

Bo Liu¹, Chengxin Yang², and Fan Li¹

¹Department of Statistical Science, Duke University, Durham NC 27708

²Department of Biostatistics and Bioinformatics, Duke University, Durham NC 27710

February 17, 2026

Abstract

This paper investigates the theoretical foundation and develops analytical formulas for sample size and power calculations for causal inference with observational data. By analyzing the variance of an inverse probability weighting estimator of the average treatment effect, we decompose the power calculation into three components: propensity score distribution, potential outcome distribution, and their correlation. We show that to determine the minimal sample size of an observational study, in addition to the standard inputs in the power calculation of randomized trials, it is sufficient to have two parameters, which quantify the strength of the confounder-treatment and the confounder-outcome association, respectively. For the former, we propose using the Bhattacharyya coefficient, which measures the covariate overlap and, together with the treatment proportion, leads to a uniquely identifiable and easily computable propensity score distribution. For the latter, we propose a sensitivity parameter bounded by the R-squared statistic of the regression of the outcome on covariates. Our procedure relies on a parametric propensity score model and a semiparametric restricted mean outcome model, but does not require distributional assumptions on the multivariate covariates. We develop an associated R package **PSpower**.

Keywords: Causal inference; Observational study; Overlap; Power; Sample size; Weighting

1 Introduction

Randomized controlled trials are the gold standard for causal inference. Designing randomized trials requires sample size and power calculations, in which investigators pre-specify a target estimand—typically the effect size of a treatment—and characteristics of the sample of the intended study. The goal is to determine the minimal sample size needed to achieve the statistical power (β), given a type I error rate (α) level, to test the treatment effect estimated by a specific method based on a sample that satisfies these characteristics, or conversely, to determine the power to detect a treatment effect at the α level given a fixed sample size. Sample size and power calculations are the two sides of the same coin, and we will use them interchangeably henceforth. Power calculation is conducted in the design stage of a study, prior to data collection. Thus, individual data are usually unavailable; investigators at best have some summary information from previous similar studies, e.g. effect sizes. Analysts must rely on this limited summary information to approximate the

full data structure. The power calculation for randomized trials is largely simplified due to randomization and has been well established (Chow et al., 2017; Branson et al., 2024).

When randomized trials are not feasible due to logistical or ethical constraints, researchers are increasingly using observational data to emulate randomized trials. The power analysis for observational studies is challenging and has been less developed. In randomized trials, there is no confounding due to randomization; therefore, one can simply use the difference in mean outcomes between arms to estimate treatment effects. Closed-form formulas, e.g., based on the two-sample z-test, are readily applicable for sample size calculation. In contrast, in observational studies, confounding must be adjusted for to obtain an unbiased estimate of treatment effects. Applying power calculation formulas designed for randomized trials to observational studies often leads to severely underpowered studies. In practice, a general power analysis method is to use simulations to generate individual data based on pre-specified summary statistics (Mukherjee et al., 2003; Qin, 2024). This method usually requires unverifiable assumptions of the entire data generating process and lacks a theoretical basis on what summary statistics are sufficient or necessary. In fact, many different data generating models may satisfy the same summary statistics but lead to vastly different sample sizes; choosing between these models is usually *ad hoc*. Another method is to use the variance inflation factor (Hsieh and Lavori, 2000; Shook-Sa and Hudgens, 2022) to approximate the inflation in the sample size of an observational study compared to a randomized trial. For example, Shook-Sa and Hudgens (2022) derived a variance inflation factor formula based on the analysis of the variance of an inverse probability weighting estimator of the average treatment effect; however, their formula requires knowledge on the distribution of the weights, which is usually not available.

In summary, existing power calculation methods usually require information on the data generating process or the distributions of the weights or covariates, which is not always available in the design stage of a study. In this paper, we bypass this limitation by reducing the variance formula to a function of a few interpretable and commonly available summary parameters instead of the weights or covariates. Based on the analysis of variance of the Hájek inverse probability weighting estimator, we decompose the power calculation into three components: propensity score distribution, potential outcome distribution, and their correlation. We show that to determine the minimal sample size of an observational study, in addition to the standard inputs in the power calculation of a randomized trial, it is sufficient to have two parameters, which quantify the strength of the confounder-treatment and the confounder-outcome association, respectively. For the former, we propose using the Bhattacharyya coefficient, which measures the covariate overlap and, together with the treatment proportion, leads to a uniquely identifiable and easily computable propensity score distribution. For the latter, we propose a sensitivity parameter bounded by the R-squared statistic of the regression of the outcome on covariates. Our derivation relies on a parametric logistic probability score model and a semiparametric restricted mean outcome model with homogeneous treatment effect. However, by appealing to the Lyapunov-type Central Limit Theorem, we bypass specific distributional assumptions on the multivariate covariates. We derive analytical formulas for three common causal estimands: the average treatment effect for the overall (ATE), treated (ATT), and overlapped population (ATO). Simulations suggest that our formula is robust under treatment heterogeneity. We develop an associated R package `PSpower`, available at <https://CRAN.R-project.org/package=PSpower>.

2 Variance and sample size based on the Hájek estimator

Suppose we have a sample of N units. Each unit i ($i = 1, 2, \dots, N$) has a binary treatment indicator Z_i , with $Z_i = 0$ being the control and $Z_i = 1$ being treated, and a vector of p covariates $X_i = (X_{1i}, \dots, X_{pi})'$. For each unit i , there are two potential outcomes $\{Y_i(1), Y_i(0)\}$ mapped to treatment and control status, of which only the one corresponding to the observed treatment is observed, denoted by $Y_i = Z_i Y_i(1) + (1 - Z_i) Y_i(0)$; the other potential outcome is missing. The propensity score is the probability of a unit being assigned to the treatment group given the covariates (Rosenbaum and Rubin, 1983): $e(x) = \Pr(Z_i = 1 \mid X_i = x)$.

The goal is to use the sample to estimate the average treatment effect (ATE):

$$\tau^{\text{ATE}} = \mathbb{E}\{Y_i(1) - Y_i(0)\} = \mathbb{E}_x\{\tau(x)\}, \quad (1)$$

where $\tau(x) = \mathbb{E}\{Y_i(1) - Y_i(0) \mid X_i = x\}$ is the conditional average treatment effect at covariate value x . To identify τ^{ATE} , we assume SUTVA (Rubin, 1980) and maintain the two standard assumptions: (i) unconfoundedness, $\Pr(Z_i \mid Y_i(0), Y_i(1), X_i) = \Pr(Z_i \mid X_i)$; (ii) overlap, $0 < \Pr(Z_i = 1 \mid X_i) < 1$. Among the consistent estimators of τ^{ATE} , we focus on the Hájek inverse probability weighting estimator for analytical simplicity:

$$\hat{\tau}_N = \frac{\sum_{i=1}^N Y_i Z_i / e(X_i)}{\sum_{i=1}^N Z_i / e(X_i)} - \frac{\sum_{i=1}^N Y_i (1 - Z_i) / \{1 - e(X_i)\}}{\sum_{i=1}^N (1 - Z_i) / \{1 - e(X_i)\}}. \quad (2)$$

Lunceford and Davidian (2004) show that $N^{1/2}(\hat{\tau}_N - \tau^{\text{ATE}})$ is asymptotically normal with variance

$$V = \mathbb{E} \left[\frac{[Y(1) - \mathbb{E}\{Y(1)\}]^2}{e(X)} \right] + \mathbb{E} \left[\frac{[Y(0) - \mathbb{E}\{Y(0)\}]^2}{1 - e(X)} \right]. \quad (3)$$

In observational studies, the true propensity score is unknown and is replaced by an estimated one. Lunceford and Davidian (2004) show that the asymptotic variance of the Hájek estimator with the propensity score estimated from a parametric model, V_0 , is V subtracted by a complex quadratic term and therefore smaller. Calculation of the quadratic term usually requires individual data, which is unavailable in power calculations. Therefore, we will proceed with V henceforth, noting that it leads to a conservative (i.e. over-estimated) sample size estimate than that based on V_0 . We investigate the discrepancy between V and V_0 using simulations in Section 5. Besides the inverse probability weighting estimators, other two classes of estimators of τ^{ATE} are the outcome regression and doubly-robust estimators. However, asymptotic variances of these estimators depend on the specific outcome model, which is infeasible to pre-specify in the stage of power analysis. In contrast, as shown later, the Hájek estimator requires much weaker assumptions on the outcome model.

With a fixed value of V , a $(1 - \alpha)$ confidence interval for $\hat{\tau}_N$ is $\hat{\tau}_N \pm z_{1-\alpha/2} V^{1/2} N^{-1/2}$, where $z_{1-\alpha/2}$ is the $(1 - \alpha/2)$ quantile of the standard normal distribution. Without loss of generality, we consider a one-sided level- α test for the null hypothesis $H_0 : \tau = 0$ against the alternative $H_a : \tau > 0$:

$$\text{reject } H_0 \text{ if } \hat{\tau}_N > z_{1-\alpha} (V/N)^{1/2}. \quad (4)$$

Standard derivation shows the minimal sample size N to reach a desired power β for a level- α test (4) with a fixed variance V is (the proof is relegated to Appendix A.1):

$$N = \tau^{-2} \left(z_{1-\alpha} V^{1/2} - z_{1-\beta} V_0^{1/2} \right)^2 \leq \tau^{-2} V (z_{1-\alpha} + z_\beta)^2, \quad (5)$$

assuming $\alpha < 0.5$ and $\beta > 0.5$, which commonly holds in practice.

In a randomized experiment, the propensity score is fixed and known, equalling the treatment proportion r , so V simplifies to $\mathbb{V}\{Y(1)\}/r + \mathbb{V}\{Y(0)\}/(1-r)$. Moreover, $\Pr\{Y(z)\} = \Pr(Y | Z = z)$, and thus the variance of the potential outcomes $Y(z)$ can be estimated by the sample variances of the outcome in arm z , s_z^2 . Following the convention, we impose $s_0 = s_1 = s$ and define the effect size as $\tilde{\tau} = \tau/s$. Then, to detect an effect size $\tilde{\tau}$ in a randomized experiment using a one-sided level- α test (4) with power β , the minimal sample size is

$$N = \left(\frac{s_1^2}{r} + \frac{s_0^2}{1-r} \right) \frac{(z_{1-\alpha} + z_\beta)^2}{\tau^2} = \frac{(z_{1-\alpha} + z_\beta)^2}{r(1-r)\tilde{\tau}^2}. \quad (6)$$

This coincides with the standard sample size formula of a two-sample z -test.

In observational studies, power calculation is more complicated because (i) the propensity scores $e(X)$ are not known, (ii) $\Pr(Y(z)) \neq \Pr(Y | Z = z)$ due to confounding, and thus the terms involving potential outcomes, $\mathbb{E}\{Y(z)\}$ and $\mathbb{V}\{Y(z)\}$, deviate from their observed counterparts $\mathbb{E}(Y | Z = z)$ and $\mathbb{V}(Y | Z = z)$, and (iii) the numerator and denominator inside the expectation operator in (3) can not be separated because the potential outcomes may be dependent on the propensity scores. When sampled units are available, we can readily address these complications. However, power calculation is conducted prior to data collection, with at best limited summary information to estimate the propensity scores or calculate the expectations.

3 Sample size and power calculation

The essence of power calculation lies in computing the variance V in (3). If we could observe (X_i, Z_i, Y_i) for each sampled unit i , V could easily be estimated by sample moments, but not so with only summary data. To determine which summary information is sufficient for computing V , we rewrite the terms in expression (3) as (taking $z = 1$ for example),

$$\mathbb{E} \left[\frac{[Y(1) - \mathbb{E}\{Y(1)\}]^2}{e(X)} \right] = \mathbb{E} [[Y(1) - \mathbb{E}\{Y(1)\}]^2] \mathbb{E} \left\{ \frac{1}{e(X)} \right\} + \text{Cov} \left[[Y(1) - \mathbb{E}\{Y(1)\}]^2, \frac{1}{e(X)} \right].$$

This expression suggests that we need three components: the propensity score distribution, the potential outcome distribution, and their correlation. We study each component in detail below.

3.1 Normal approximation of linear combinations of covariates

Both the propensity score and the outcome models are commonly specified as a generalized linear model with a linear combination of covariates, $X'\beta = \sum_{j=1}^p \beta_j X_j$, as the predictor. However, in power calculations, we usually do not have specific information on each covariate. Previous authors often operated with a single normal predictor (e.g. Raudenbush, 1997; Kelcey et al., 2017), but without theoretical justification. Here we invoke a special case of the Lyapunov Central Limit Theorem (Billingsley, 1995) to approximate the distribution of the scalar summary $X'\beta$ and thus justify such a procedure.

Theorem 1. *Assume X_1, X_2, \dots is a sequence of independent random variables with mean 0 and variance 1. Let β_1, β_2, \dots be a sequence of real numbers. If the following two conditions hold: (i) there exists a positive number B such that $\mathbb{E}(X_j^4) < B$, and (ii) $\max_{1 \leq j \leq p} \beta_j^2 (\sum_{j=1}^p \beta_j^2)^{-1} = o(1)$, then*

$$\frac{1}{\sum_{j=1}^p \beta_j^2} \sum_{j=1}^p \beta_j X_j \Rightarrow \mathbf{N}(0, 1). \quad (7)$$

The proof is relegated to Appendix A.2. Condition (i) ensures that the distribution of each covariate does not have heavy tails, and condition (ii) ensures that no single covariate dominates the linear combination. Theorem 1 suggests that, under Condition (i)-(ii), the linear combination $X'\beta$ converges to a Normal distribution as the number of covariates (p) increases. In practice, some covariates might be correlated and p might be modest. Some versions of the central limit theorem for dependent variables can be invoked when there is known correlation structure between covariates. However, in the context of power analysis, such information is usually not available and, in fact, analysts would avoid making specific assumptions about the covariate distributions. Instead, we conducted extensive simulations to examine the empirical distribution of $X'\beta$ under a wide range of scenarios. These simulations show $X'\beta$ approximates a Normal distribution satisfactorily often with as few as 10 variables as long as there is no strong pairwise correlation between X . We also draw the empirical distribution of $X'\beta$ in four real applications, including the benchmark RHC data used in Section 5.3, with p between 10 to 50, each of which also exhibits normality (details in Appendix B.1). Importantly, our derivation in the following sections only relies on the normality of $X'\beta$ rather than the exact distribution, which is easier to achieve with a modest p and mild correlation between covariates.

3.2 Distribution of propensity scores

This subsection shows how to, under a logistic model specification, uniquely identify the distribution of propensity scores with only two parameters: the treatment proportion r and an overlap coefficient ϕ that measures the similarity of covariates between two groups. The key idea is to approximate the distribution of propensity scores by a computationally tractable Beta distribution, as elaborated below.

Following the literature, we impose a logistic regression model for the propensity scores: $e(X) = \text{expit}(W_e)$, where $W_e = \beta_0 + \sum_{j=1}^p \beta_j X_j$. Theorem 1 motivates us to approximate the distribution of the scalar summary W_e by a Normal distribution $\mathbf{N}(\mu_e, \sigma_e^2)$, and thus approximate the propensity score distribution by a logit-normal distribution $\mathcal{P}(\mu_e, \sigma_e^2)$.

To determine the two parameters μ_e and σ_e of the logit-normal distribution, we would need to impose constraints in the form of summary information about the treatment assignment. The first constraint, which is almost always available, is the proportion of the treatment group in the intended study: $r = \Pr(Z_i = 1)$. The second constraint is a measure, denoted as ϕ , of the similarity between the covariate distributions in the treatment and control groups, $\Pr(X | Z = 1)$ versus $\Pr(X | Z = 0)$. There are many choices of the specification of ϕ ; important selection criteria include: (i) there should be 1-1 map between (r, ϕ) and (μ_e, σ_e) so that the data generating process of the propensity score is unique, and (ii) easy to compute the propensity score distribution given (r, ϕ) .

The logit-normal distribution does not have a closed-form mean and thus it is generally difficult to solve for (μ_e, σ_e) given (r, ϕ) . Instead, we propose to approximate the logit-normal distribution by a Beta distribution, which also has a range on $[0, 1]$ and is easy to compute. Applying the method in Aitchison and Shen (1980), we can derive the ‘‘optimal’’ Beta distribution approximation of a logit-normal distribution by minimizing the Kullback-Leibler divergence between them. Specifically, for a logit-normal distribution $\mathcal{P}(\mu_e, \sigma_e^2)$ and its optimal Beta distribution approximation $\text{Beta}(a, b)$, their parameters satisfy

$$\mu_e = \psi(a) - \psi(b), \quad \sigma_e^2 = \psi'(a) + \psi'(b) \tag{8}$$

where ψ and ψ' are the digamma and trigamma functions, respectively. Numerical examples in Appendix B.2 illustrate that this approximation is accurate for a wide range of logit-normal distributions.

If $e(X) \sim \text{Beta}(a, b)$, then there is a closed-form relation between a, b, r : $r = a/(a + b)$. Therefore, it suffices to identify the propensity score distribution if we find another easily computable relation between a, b and the overlap measure ϕ . The question now becomes how to specify such a ϕ . Directly operating on the multivariate covariate X is challenging; instead we operate on the propensity score $e(X)$, which is the coarsest balancing score (Rosenbaum and Rubin, 1983). Let $f_z(u)$ be the density of $e(X)$ in arm z : $f_z(u) = \Pr(e(X) = u \mid Z = z)$. We propose to use the Bhattacharyya coefficient (Bhattacharyya, 1943) to measure the covariate overlap between two arms:

$$\phi \equiv \int_0^1 \sqrt{f_1(u)f_0(u)} \, du. \quad (9)$$

The Bhattacharyya coefficient ϕ satisfies $0 \leq \phi \leq 1$, with $\phi = 0$ if and only if the support of f_0 and f_1 does not overlap, whereas $\phi = 1$ if and only if $f_0 = f_1$ almost everywhere. Therefore, ϕ is an appropriate measure of overlap; we term it as the *overlap coefficient* hereafter. We choose the Bhattacharyya coefficient because it has a major computable advantage in our context, established in the following proposition.

Proposition 1. For $e(X) \sim \text{Beta}(a, b)$ with $(a > 0, b > 0)$:

(i) the overlap coefficient ϕ has a closed-form expression as a function of (a, b) :

$$\phi = \frac{\Gamma(a + 0.5) \Gamma(b + 0.5)}{a^{1/2}\Gamma(a) b^{1/2}\Gamma(b)}; \quad (10)$$

(ii) given r , ϕ is monotonically increasing in both a and b ;

(iii) there is a 1-1 map (bijection) between (r, ϕ) and (a, b) .

The proof of (i)-(iii) is relegated to Appendix A.3-A.5, respectively. Proposition 1 establishes that, given (r, ϕ) , we can obtain the Beta parameters (a, b) by solving two equations: (i) $r = a/(a + b)$, and (ii) Equation (10). Furthermore, we can use the bisection method to solve for (a, b) efficiently, based on which we reverse the Beta approximation of $e(X)$ to obtain the logit-normal distribution parameters (μ_e, σ_e) . It is worth noting that other specification of the overlap coefficient, e.g. the overlapping area between the density functions of two distributions (Inman and Bradley, 1989), usually does not lead to a closed-form expression of ϕ as a function of (a, b) , which is crucial for verifying the 1-to-1 map between (r, ϕ) and (a, b) .

For $e(x) \sim \text{Beta}(a, b)$, we can use the Bayes theorem to show that $\Pr(e(x) \mid Z = 1) \sim \text{Beta}(a + 1, b)$ and $\Pr(e(x) \mid Z = 0) \sim \text{Beta}(a, b + 1)$. Figure 1 shows the overlaying distributions of $e(X)$ in the $Z = 1$ and $Z = 0$ groups corresponding to different combinations of (r, ϕ) . Theoretically, the overlap coefficient ϕ is between 0 and 1. However, Figure 1 shows that there is little difference between the propensity score distribution if $\phi < 0.8$, especially when $r < 0.5$, which is the common scenario in observational studies. Further visual check (details omitted) reveals that, when $\min\{a, b\} < 1$, the Beta distribution is U-shaped and the propensities are concentrated in the tail region (close to 0 or 1), suggesting extremely poor overlap between groups. Calculations shows $a = b = 1, 1.5, 2.5, 5$ corresponding to $\phi = 0.80, 0.85, 0.90, 0.95$, respectively. Therefore, we set a simple heuristic rule of thumb for measuring the degree of overlap: $\phi < 0.8, \in (0.8 - 0.9), \in (0.9 - 0.95), > 0.95$ corresponds to very poor, poor, moderate, good overlap, respectively. In practice, users could compute ϕ from a pilot study, of which we provide a computational method in Appendix B.3. When a pilot study is not available, we recommend users to conduct sensitivity analysis on a range of ϕ valued based on domain knowledge.

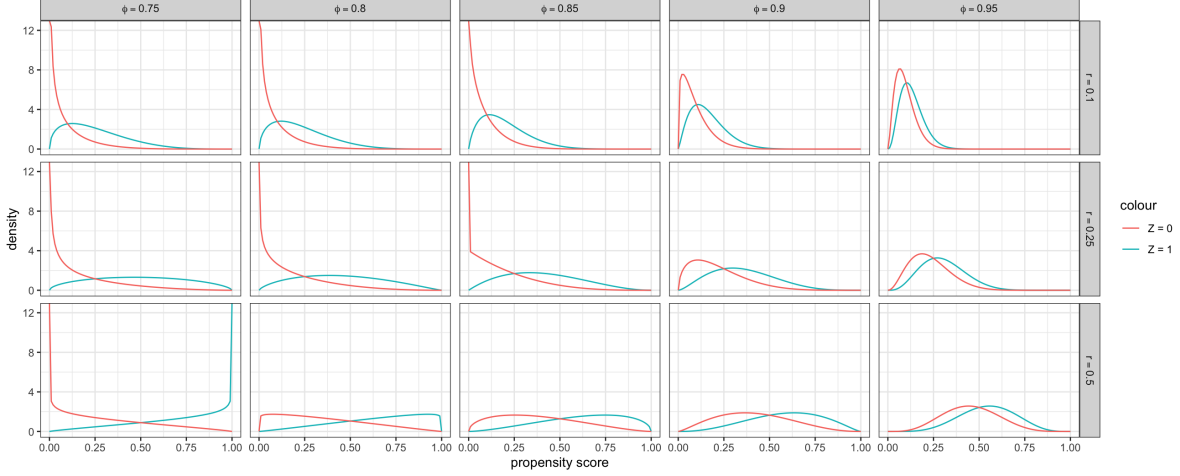


Figure 1: Distributions of $e(X)$ of the treatment and control groups corresponding to different combinations of (r, ϕ) , where $e(X)$ follows a $\text{Beta}(a, b)$ distribution with a and b determined by (r, ϕ) .

3.3 Distribution of potential outcomes

This subsection shows how to relate potential outcomes to propensity scores under mild model assumptions. The key idea is to project the outcomes into the space spanned by the scalar summary of the propensity score obtained in Section 3.2.

We assume a restricted mean model (RMM) with a homogeneous treatment effect τ for the potential outcomes

$$Y(z) = f(X) + z\tau + \epsilon. \quad (11)$$

Furthermore, we assume (i) homoscedasticity of the error, $\mathbb{V}\{\epsilon \mid e(X)\} = \mathbb{V}(\epsilon)$, and (ii) $f(X)$ and W_e are jointly Normal. We do not impose additional distributional assumptions on $Y(z)$ or ϵ . The homoscedasticity assumption states that the propensity score is not predictive of the error variance of potential outcomes; it is weaker than the canonical version $\mathbb{V}(\epsilon \mid X) = \mathbb{V}(\epsilon)$. The Normal assumption holds under various models for $f(X)$, most straightforwardly under a linear model $f(X) = \gamma_0 + \sum_{j=1}^p \gamma_j X_j$. Specifically, with a linear $f(X)$, we can approximate the joint distribution of W_e and $f(X)$ by a bivariate normal distribution, invoking a multivariate extension of the Lyapunov central limit theorem (Bentkus, 2005). More generally, when $f(X)$ is itself an approximately normal function of covariates—as is often the case when no single covariate dominates as specified in Theorem 1—the joint normality provides a reasonable approximation. We evaluate the empirical performance of our method under this assumption using simulations in Section 5.

Under the joint normality of $f(X)$ and W_e , the correlation between the potential outcomes and the propensity score is captured by the correlation between $f(X)$ and W_e . Therefore, we decompose $f(X)$ into two parts, one collinear with W_e and the other orthogonal to W_e : $f(X) = aW_e + W_e^\perp$ such that $\text{cov}(W_e, W_e^\perp) = 0$. Then, the potential outcomes can be expressed as $Y(z) = aW_e + W_e^\perp + z\tau + \epsilon$, where W_e^\perp is independent of W_e because (W_e, W_e^\perp) is jointly Normal. By the definition of RMM, ϵ is also uncorrelated with any function of X , including W_e . Therefore, with a slight abuse of notation, we denote the compound error $W_e^\perp + \epsilon$ as ϵ .

The key quantity in the asymptotic variance of the Hájek estimator, $Y(z) - \mathbb{E}\{Y(z)\}$, now reduces to $a\{W_e - \mathbb{E}(W_e)\} + \{\epsilon - \mathbb{E}(\epsilon)\}$ for $z = 0, 1$, whose mean and variance are fully characterized by two unknown parameters, a and $\sigma_y^2 = \mathbb{V}(\epsilon)$. To solve the parameters, we would need two inputs and constraints. It is natural

to set the variance of potential outcomes in the corresponding group as an input, $S^2 \equiv \mathbb{V}\{Y(0)\} = \mathbb{V}\{Y(1)\}$. For the other input, we use the correlation between the linear component of the propensity scores W_e —a summary of covariates—and the potential outcomes, i.e., $\rho \equiv \text{cor}\{Y(1), W_e\} = \text{cor}\{Y(0), W_e\}$. With the specified values (S^2, ρ) , one can solve for the unknown parameters (a, σ_y^2) by the following equations (the proof is relegated to Appendix A.6)

$$a = \rho|S|\sigma_e^{-1}, \quad \sigma_y^2 = (1 - \rho^2)S^2. \quad (12)$$

We now interpret the seemingly opaque correlation parameter ρ under homogeneous treatment effect. Recall that the propensity score $e(X) = \text{expit}(W_e)$; therefore, W_e is a scalar summary of the covariates that are predictive of treatment assignment. Because confounders are covariates that are correlated with both treatment and outcome, we interpret ρ as a measure of the confounder-outcome association: as ρ increases, confounding covariates exert a greater influence on the outcome between treatments. The parameter ρ is intrinsically related to a standard and interpretable quantity: the covariate-outcome association, $R = \text{cor}\{Y(0), f(X)\}$, which measures the extent to which the outcome is driven by the covariates rather than noise. In fact, R^2 is equivalent to the R-squared statistic on the potential outcome: $\mathbb{V}\{f(X)\} / \mathbb{V}\{Y(0)\}$. Furthermore, we derive the following expression to show that $|\rho|$ is bounded by $|R|$:

$$\rho^2 = \left[\frac{\text{cov}\{Y(0), W_e\}}{\{\mathbb{V}(W_e)\}^{1/2}[\mathbb{V}\{f(X)\}]^{1/2}} \right]^2 \frac{\mathbb{V}\{f(X)\}}{\mathbb{V}\{Y(0)\}} = \text{cor}^2\{f(X), W_e\}R^2 \leq R^2. \quad (13)$$

In completely randomized trials, covariates are independent of the treatment assignment by design, so that W_e reduces to a constant, and therefore $\text{cor}(f(X), W_e) = 0$ and $\rho = 0$. In observational studies, as the covariates associated with propensity scores overlap more with the covariates associated with potential outcomes, $\text{cor}(f(X), W_e)$ will get farther away from 0. Equation (13) implies that users can bound ρ^2 by the R-squared value encoding the proportion of the variance of potential outcomes explainable by covariates, of which investigators often have an educated guess based on prior domain knowledge. Li et al. (2018b) used the same R-squared statistic to quantify covariate-outcome association. In practice, one might estimate $|\rho|$ from a pilot study, or conduct a sensitivity analysis of $|\rho|$ in the range of $(0, |R|)$ based on domain knowledge, or simply set $\rho = 0$ though it could lead to a mild underestimate of the sample size.

3.4 Analytical formula for sample size calculation

In this subsection, we will build on Section 3.2-3.3 to derive an analytical sample size calculation formula. Following the convention of power analysis, we define the effect size as the treatment effect standardized by the standard error: $\tilde{\tau} = \tau/S$. The following theorem presents the analytical formula for the sample size calculation of τ^{ATE} (the proof is relegated to Appendix A.7).

Theorem 2. *Let $\tilde{\tau}$ be the desired standardized effect size of the ATE. The minimum sample size for the one-sided level- α test defined in (4) for detecting $\tilde{\tau}$ with power β is $N = \tilde{V} (z_{1-\alpha} + z_\beta)^2 / \tilde{\tau}^2$, with*

$$\tilde{V} = 2 \left\{ 1 + (\rho^2 \sigma_e^2 + 1) \exp\left(\frac{\sigma_e^2}{2}\right) \cosh(\mu_e) \right\}, \quad (14)$$

where $\cosh(\mu_e) = \{\exp(\mu_e) + \exp(-\mu_e)\}/2$.

The minimum sample size for the two-sided counterpart of test (4) is obtained by replacing $z_{1-\alpha}$ with

$z_{1-\alpha/2}$ in Theorem 2. Equation (14) shows that the variance \tilde{V} only involves μ_e and σ_e^2 , both of which can be derived from the distribution of $e(X)$ that is determined by (r, ϕ) , and ρ . This simplification reduces the number of inputs for the sample size calculation to two, namely (ϕ, ρ) , in addition to the standard $\tilde{\tau}, \alpha, \beta, r$. In the special case of a randomized trial, $\rho = 0$, and the minimal sample size reduces to formula (6). Based on Equation (14) and jointly with Proposition 1(ii) and the relation in (8), the following corollary on the relationship between N and (ρ, ϕ) is immediate.

Corollary 1. *The variance \tilde{V} and thus the sample size N (i) monotonically increases in $|\rho| \in (0, 1]$ given (r, ϕ) , and (ii) monotonically decreases in $\phi \in (0, 1]$ given r .*

Figure 2 shows a flow chat of how to decompose the variance of the Hájek estimator into three components and compute each component from the proposed inputs.

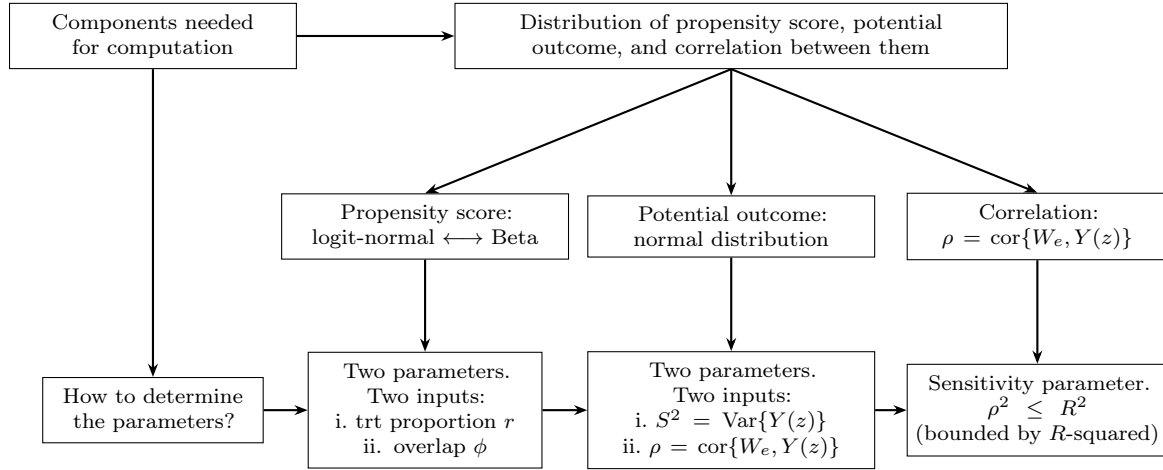


Figure 2: Flow chat of decomposing and computing the variance of the Hájek estimator from summary inputs.

Remark 1. In summary, our derivation relies on (i) a logistic model for the propensity scores, and (ii) a semiparametric homoscedastic restricted mean outcome model with a homogeneous treatment effect. In real applications, the true data generating process might deviate from the assumptions. In particular, heterogeneous treatment effects are common. We can extend the homogeneous outcome model (11) to a varying coefficient model to accommodate heterogeneity: $Y(z) = f(X) + z\tau(X) + \epsilon$, where $\tau(X)$ stands for the conditional average treatment effect at covariate X . Maintain the homoscedasticity and joint normality assumptions and use the same projection to the space spanned by W_e as in the homogeneity model. Then, simple algebra (details are omitted) shows that the asymptotic variance of the Hájek estimator V of the heterogeneity model depends on the variance of $\tau(X)$, the knowledge of which is generally not available before data collection as in power analysis. This challenge is also discussed in the context of sample size calculation for rerandomization (Branson et al., 2024). Instead, we use simulations in Section 5 to examine consequences of violation to homogeneity and find Formula (14) is generally robust.

Remark 2. Our analytical derivation elucidates the connection and distinction between power calculations in randomized trials and observational studies. Specifically, both cases require four parameters: α, β , the standardized effect size $\tilde{\tau}$, and the treatment proportion r . Observational studies require two additional inputs: the overlap coefficient ϕ and the correlation parameter ρ^2 , both of which have a natural interpretation. This result is intuitive because the key difference between observational studies and randomized trials is the presence of confounders in the former, which are pre-treatment covariates that affect the treatment assignment

and the outcome simultaneously. The parameters ϕ and ρ^2 quantify the strength of confounder-treatment and confounder-outcome association, respectively. A similar strategy is used in the formulation of the E-value (Ding and VanderWeele, 2016). Intuitively, as the covariate overlap between groups (encoded by ϕ) decreases and the correlation between covariates and the outcome (encoded by ρ^2) increases, an observational study deviates further from a randomized trial, rendering the marginal distribution of the observed outcomes deviate further from that of the potential outcomes and thus require more sample units to identify the causal estimands. This matches Corollary 1.

Remark 3. The sample size formula in Shook-Sa and Hudgens (2022), derived based on a variance inflation factor, is a special case of formula (14). Specifically, assuming $e(X) \sim \text{expit}(\mathbf{N}(\mu_e, \sigma_e^2))$, their formula becomes $\tilde{V}_{\text{SH}} = 2 \{1 + \exp(\sigma_e^2/2) \cosh(\mu_e)\}$. Comparing to formula (14), we have $\tilde{V} = \tilde{V}_{\text{SH}} + 2\rho^2\sigma_e^2 \exp(\sigma_e^2/2) \cosh(\mu_e)$. Therefore, \tilde{V}_{SH} equals \tilde{V} when $\rho = 0$ and is smaller than \tilde{V} otherwise. Although ρ^2 is small in many of our simulation studies, ignoring it risks underestimating the sample size in general settings. Shook-Sa and Hudgens (2022) discussed a term that implicitly adjusts for the confounder-treatment association, but it is not estimable without prior data on both weights and outcomes.

Remark 4. For binary outcomes, because the mean of a Bernoulli distribution determines the variance, compared to continuous outcomes in Section 3.3, we have two fewer constraints to determine the outcome distribution. As a simple solution, we recommend using linear models for binary outcomes so that the proposed method directly applies. Numerical examples in Section 5.3 and Appendix C.1 suggest that this approach generally works well in practice.

4 Weighted average treatment effect estimands

In the presence of poor overlap between the treatment groups, the inverse probability weighting can lead to excessive variance due to extreme propensity scores. Alternative weighting schemes are often more desirable. In this section, we extend the above methodology to a general class of weighted average treatment effect (WATE). Assume that the observed sample is drawn from a population with covariates distribution $f(x)$, and let $f(x)h(x)$ denote the covariate distribution of a *target population*, where $h(x)$ is called a tilting function. Then, we can represent the average treatment effect on that target population using a WATE

$$\tau^h = \frac{\mathbb{E}[\tau(x)h(x)]}{\mathbb{E}[h(x)]}. \quad (15)$$

When $h(x) = 1$, τ^h reduces to ATE; when $h(x) = e(x)$, τ^h becomes the average treatment effect for the treated (ATT); when $h(x) = e(x)(1 - e(x))$, τ^h becomes the average treatment effect for the overlap population (ATO). We can use a unified weighting strategy to identify the WATE because $\tau^h = \mathbb{E}[w_1(X)ZY - w_0(X)(1 - Z)Y]$, where $w_1(x) = h(x)/e(x)$, $w_0(x) = h(x)/(1 - e(x))$ (Li et al., 2018a). This corresponds to (i) the inverse probability weight (IPW), ($w_1 = 1/e(x)$, $w_0 = 1/(1 - e(x))$), for the ATE; (ii) the ATT weight, ($w_1 = 1$, $w_0 = e(x)/(1 - e(x))$), for the ATT; and (iii) the overlap weight (OW), ($w_1 = 1 - e(x)$, $w_0 = e(x)$), for the ATO.

The Hájek estimator for the WATE is:

$$\hat{\tau}_w = \frac{\sum_i w_1(X_i)Z_i Y_i}{\sum_i w_1(X_i)Z_i} - \frac{\sum_i w_0(X_i)(1 - Z_i)Y_i}{\sum_i w_0(X_i)(1 - Z_i)}. \quad (16)$$

We can adapt the procedures in Section 3 to derive sample size calculation formulas for the ATT and ATO estimands. Specifically, the procedures to determine the propensity score and the outcome distributions

remain the same, but the variance formula changes. Unlike the ATE, there is no deterministic order between the variance of the Hájek estimator with the estimated versus true propensity score for other WATE estimands (Yang and Ding, 2018). For the same reasons as with the ATE stated in Section 2, we choose to proceed with the variance with the true e .

We show the variance of the Hájek estimator for the WATE with the tilting function h is:

$$V_w \equiv \mathbb{V}(\hat{\tau}_w) = \frac{1}{\mathbb{E}[h(X_i)^2]} \mathbb{E} \left[\left\{ \frac{(Y_i(1) - \xi_1)^2}{e(X_i)} + \frac{(Y_i(0) - \xi_0)^2}{1 - e(X_i)} \right\} h(X_i)^2 \right], \quad (17)$$

where $\xi_z = \mathbb{E}_h[Y_i(z)] = \mathbb{E}[h(X_i)Y_i(z)]/\mathbb{E}[h(X_i)]$; the proof is relegated to Appendix A.8. For the ATE, $h(X_i) = 1$, and V_w reduces to V as in Equation 3. For the ATT and ATO, $h(X_i)$ is a function of $e(X_i)$ and thus V_w is also fully determined by the joint distribution of $e(X_i)$ and the potential outcomes $Y_i(z)$, which can be computed as in Sections 3.2 and 3.3. However, neither the ATT or the ATO has a closed-form expression of variance, but they can be computed numerically.

We outline how to compute V_w with the tilting function $h(X)$ given the parameters (μ_e, σ_e) and (a, σ_y^2) . For the ATT and ATO, $h(X)$ is a function of the propensity score $e(X)$, whose distribution can be approximated by W_e . Therefore, we can also write the tilting function as $h(W_e) = \text{expit}(W_e)$ for ATT and $h(W_e) = \text{expit}(W_e)[1 - \text{expit}(W_e)]$ for ATO, such that $h(W_e)$ has approximately the same distribution as $h(X)$. Calculating the denominator $\mathbb{E}[h(X)^2] = \mathbb{E}[h(W_e)^2]$ where $W_e \sim \mathcal{N}(\mu_e, \sigma_e^2)$ involves numerically (*e.g.* Simpson's method) evaluating the following integral

$$\int_{-\infty}^{\infty} h(u)^2 \frac{1}{\sqrt{2\pi\sigma_e^2}} \exp\left(-\frac{(u - \mu_e)^2}{2\sigma_e^2}\right) du, \quad (18)$$

which is available in most statistical software. For the numerator, we show that

$$\mathbb{E} \left[\frac{(Y_i(1) - \xi_1)^2}{e(X_i)} h(X_i)^2 \right] \quad (19)$$

$$= a^2 \mathbb{E} \left[\left(W_e - \frac{\mathbb{E}[h(W_e)W_e]}{\mathbb{E}[h(W_e)]} \right)^2 \frac{h(W_e)^2}{\text{expit}(W_e)} \right] + \sigma_y^2 \mathbb{E} \left[\frac{h(W_e)^2}{\text{expit}(W_e)} \right],$$

$$\mathbb{E} \left[\frac{(Y_i(0) - \xi_0)^2}{1 - e(X_i)} h(X_i)^2 \right] \quad (20)$$

$$= a^2 \mathbb{E} \left[\left(W_e - \frac{\mathbb{E}[h(W_e)W_e]}{\mathbb{E}[h(W_e)]} \right)^2 \frac{h(W_e)^2}{1 - \text{expit}(W_e)} \right] + \sigma_y^2 \mathbb{E} \left[\frac{h(W_e)^2}{1 - \text{expit}(W_e)} \right],$$

whose proof is relegated to Appendix A.9, where all the expectation terms only involve W_e and can hence be calculated numerically by evaluating the corresponding integrals.

5 Numerical Experiments

5.1 Synthetic Data: homogeneous treatment effect

Following the simulation design in Li et al. (2019), we simulate $N = 1,000,000$ units with 10 covariates of different types as the superpopulation. Covariates X_1 to X_4 are binary with $\text{Ber}(p)$ with $p = 0.2, 0.4, 0.6, 0.8$, respectively; $X_5 \sim \text{Unif}(0, 1)$; X_6 to X_8 follows a Poisson distribution with mean parameters 1, 2, and 3 respectively; $X_9 \sim \text{Gamma}(2, 3)$ and $X_{10} \sim \text{Beta}(2, 3)$. We generate the treatment indicator $Z \sim \text{Ber}(\text{expit}(\beta_0 + \kappa X\beta))$,

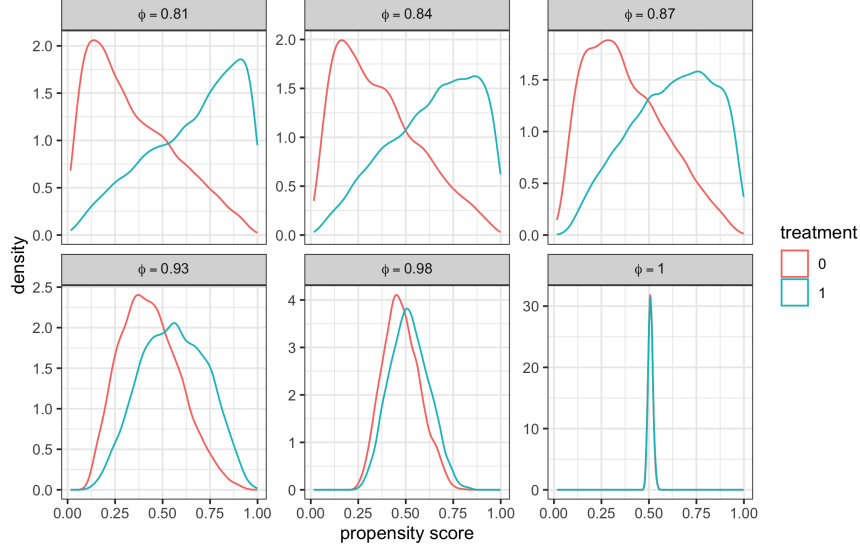


Figure 3: Distribution of the propensity scores in two treatment arms with fixed $r = 0.5$ and various overlap coefficient $\phi = 1.00, 0.98, 0.93, 0.87, 0.84, 0.81$, respectively, in Simulation 5.1.

where $\beta = (1, 1, -1, 0, -2, 1, 0.5, 0, 0, 0)'$. The parameter $\kappa \in \{0, 0.25, 0.5, 0.75, 0.9, 1\}$ controls the overlap between two treatment groups, corresponding to the overlap coefficient $\phi \in \{1.00, 0.98, 0.93, 0.87, 0.84, 0.81\}$, respectively; $\kappa = 0$ corresponds to a randomized trial. Figure 3 shows the overlap between two groups with varying κ . For these κ values, we choose $\beta_0 \in \{0, -0.248, -0.489, -0.722, -0.860, -0.951\}$ accordingly so that the treatment proportion $r = \mathbb{E}(Z) = 0.5$. We simulate from a potential outcome model with a *homogeneous treatment effect* τ : $Y(z) \sim \mathbf{N}(X\gamma + \tau z, 4^2)$, where $\gamma = (1, 1, -1, -1, 0, -1, -1, 0, 1, 1)'$ and $\tau = 1$, and let the observed outcome $Y_i = Z_i Y(1) + (1 - Z_i) Y(0)$.

We fix the power at 0.80 and solve the sample size for each value of κ . We calculate the summary statistics (r, ϕ, S, ρ) as defined in Section 3 from the $N = 1,000,000$ units in the superpopulation. The proportion of treatment, r , is fixed at 0.5. With the logistic model for the propensity score, $e(X) = \text{expit}(\beta_0 + X\beta)$, the latent variable W_e is estimated by $\hat{\beta}_0 + X\hat{\beta}$, where $(\hat{\beta}_0, \hat{\beta})$ is the estimated intercept and coefficients of the logistic regression of Z on X . Although none of the covariates X is normal, the latent linear combination of X , W_e , appears to be close to normal (see the rightmost column of Figure 5 in Appendix B.1). We calculate the pooled variance S^2 and correlation ρ empirically. To calculate ϕ , we use the empirical cumulative probability function of the propensity scores (details are relegated to Appendix B.3). We present ϕ, ρ^2, R^2 in Table 1. The R-squared statistic R^2 is obtained by fitting the linear model $Y \sim X$ to the simulated data, with Y centered within the respective treatment arm. The R^2 turns out to be much larger than ρ^2 , which is not surprising as R^2 is the theoretical upper bound of ρ^2 , and provides the most conservative estimate when there is no substantive knowledge on ρ^2 .

We use inputs (r, ϕ, ρ^2) and the standardized effect size $\tilde{\tau} = 1/S$ to inversely calculate the sample size N_{pos} . Table 1 shows the calculated sample size to achieve the nominal power 0.80 under various degrees of overlap. Then, we sample N_{pos} units randomly from the $N = 1,000,000$ units in the superpopulation. We repeat the process for $B = 10,000$ times; each time, we conduct the hypothesis test (4) at level $\alpha = 0.05$, with $\hat{\tau}_N$ calculated with true and estimated propensity scores, respectively. We then estimate the power by the proportion of the $B = 10,000$ replications where the null hypothesis is rejected. Table 1 also reports

Table 1: Sample size calculation by the proposed method, the two-sample z -test and the method in (Shook-Sa and Hudgens, 2022) to achieve nominal power of 0.80 under various degrees of overlap. The power is obtained from random sampling of the calculated size from the $N = 1,000,000$ units. The Monte Carlo error for a power of 0.8 is 0.004. The treatment proportion r is fixed at 0.5. The empirical S^2 is close to 20 in all settings.

ϕ	ρ^2	R^2	Proposed			z -test			Shook-sa & Hudgens		
			Size	True PS	Est PS	Size	True PS	Est PS	Size	True PS	Est PS
1.00	0.02	0.20	645	0.83	0.88	629	0.80	0.87	629	0.80	0.87
0.98	0.03	0.20	656	0.79	0.87	628	0.78	0.85	653	0.80	0.88
0.93	0.03	0.19	754	0.79	0.87	626	0.73	0.80	742	0.78	0.86
0.88	0.02	0.19	993	0.78	0.85	624	0.60	0.65	950	0.77	0.84
0.84	0.02	0.19	1290	0.80	0.85	623	0.48	0.53	1216	0.77	0.84
0.81	0.02	0.19	1617	0.81	0.87	622	0.40	0.45	1481	0.79	0.81

the power calculated based on Shook-Sa and Hudgens (2022) (SH). The proposed method consistently leads to powers close to the nominal 0.80; the SH method leads to slightly lower power. The similarity between the results from our method and from the SH method is as expected from Remark 3 given the small ρ^2 . As noted before, the power based on the estimated propensity scores is higher than that based on the true scores, rendering the proposed method conservative. Note that the discrepancy in variance between the true and estimated propensity scores could be magnified in the simulation compared to most real studies, because both Z and Y are drawn from the underlying true model. We also include the sample size calculated by two-sample z -test for comparison. When the overlap is perfect, the z -test correctly calculates the sample size. However, when the overlap is poor, meaning that the intended observational study is far from a target randomized trial, the z -test, which treats observational studies as randomized trials and thus ignores the degree of overlap, tends to vastly underestimate the sample size.

The parameter ρ^2 is usually unknown; we suggest treating ρ^2 as a sensitivity parameter between 0 and R^2 . For $\phi \in \{1.00, 0.98, 0.93, 0.88, 0.84, 0.81\}$, sensitivity analyses will yield sample sizes between (629, 630), (653, 669), (742, 821), (959, 1239), (1225, 1818) and (1515, 2516), respectively. The results show that when the overlap is good, *i.e.*, the observational study resembles a randomized trial, the minimal sample size is robust to the choice of ρ^2 . However, as the overlap deteriorates, the sample size becomes more sensitive to the choice of ρ^2 . This finding restates the importance of covariate overlap in observational studies and presents the challenge of sample size calculation with worse overlap. The wide intervals do not reflect a drawback of the proposed method; instead, it displays the sensitivity to the “hidden” parameter ρ^2 , which has been mostly ignored in the existing literature. Such sensitivity also highlights the importance of the bound $\rho^2 \leq R^2$, which guarantees that the sample size falls into a reasonable range with modest overlap because R^2 is often small (e.g. 0.2) in clinical studies.

We also conduct simulation studies where (i) the outcomes are binary and (ii) the estimand is the ATT or ATO, details of which are relegated to Appendix C.1 and C.2, respectively. The proposed method is shown to correctly estimate the sample size in both settings.

5.2 Synthetic Data: heterogeneous treatment effect

We extend the simulation in Section 5.1 to assess the proposed method in the presence of heterogeneous treatment effect (HTE). We generate covariates, propensity score, treatment indicator, and the control

Table 2: Sample size calculation by the proposed method, the two-sample z -test and the method in (Shook-Sa and Hudgens, 2022) to achieve nominal power of 0.80 under various degrees of overlap and HTE. The power is obtained from random sampling of the calculated size from the $N = 1,000,000$ units. The Monte Carlo error for a power of 0.8 is 0.004. The empirical S^2 is about 21.1 and 19.5 for the upper and lower panels, respectively.

ϕ	ρ^2	R^2	Proposed			z -test			Shook-Sa & Hudgens		
			Size	True PS	Est PS	Size	True PS	Est PS	Size	True PS	Est PS
<i>covariates-driven HTE</i>											
1.00	0.02	0.23	663	0.82	0.89	663	0.82	0.89	663	0.81	0.88
0.98	0.03	0.23	693	0.80	0.88	664	0.80	0.88	691	0.82	0.88
0.93	0.03	0.24	795	0.81	0.88	665	0.72	0.81	787	0.81	0.88
0.87	0.03	0.24	1048	0.81	0.87	666	0.61	0.67	1010	0.78	0.84
0.83	0.03	0.24	1363	0.80	0.85	666	0.49	0.53	1253	0.75	0.81
0.81	0.03	0.24	1715	0.79	0.84	667	0.37	0.42	1528	0.75	0.74
<i>propensity score-driven HTE</i>											
0.98	0.01	0.17	641	0.79	0.86	616	0.79	0.85	640	0.80	0.86
0.93	0.00	0.17	727	0.80	0.85	613	0.72	0.78	726	0.79	0.85
0.87	0.00	0.17	942	0.78	0.82	612	0.60	0.63	928	0.77	0.83
0.83	0.00	0.17	1207	0.78	0.82	611	0.49	0.47	1150	0.77	0.80
0.81	0.00	0.17	1499	0.73	0.78	611	0.39	0.37	1401	0.71	0.76

potential outcome $Y_i(0)$ following Section 5.1, and simulate $N = 1,000,000$ units as the superpopulation. Following the treatment effect decomposition in Ding et al. (2019), we generate the individual treatment effect as $\tau_i = \tau_0 + g(X_i) + u_i$, where $g(X_i)$ is the systematic component driven by observed covariates and $u_i \sim \mathbf{N}(0, 0.2^2)$ is the idiosyncratic component independent of observed covariates. The treated potential outcome is $Y_i(1) = Y_i(0) + \tau_i$. We target the ATE estimand $\tau = \mathbb{E}[\tau_i]$. We consider two systematic components: (i) covariate-driven HTE, where $g(X_i) = \delta(X_{1,i} + X_{9,i})$, so that treatment effect heterogeneity is driven by both a confounder and a precision variable, and (ii) propensity score-driven HTE, where $g(X_i) = \delta W_{e,i}$, so that treatment effect varies along the logit propensity score. For each scenario, we calibrate (τ_0, δ) so that $\mathbb{E}[\tau_i] = \mathbb{V}(\tau_i) = 1$ in the superpopulation, representing substantial effect heterogeneity where the standard deviation of individual treatment effects equals the true ATE. $\phi = 1$ ($\kappa = 0$) is not applicable to propensity score-driven HTE because W_e is constant, and is thus omitted. By construction, this HTE mechanism increases $\mathbb{V}[Y(1)]$ while $\mathbb{V}[Y(0)]$ remains unchanged, a feature also shared by control potential outcome-driven HTE simulation designs in Ding et al. (2015); Branson and Dasgupta (2020).

As in Section 5.1, from the superpopulation, we estimate W_e by \widehat{W}_e with a logistic model and τ by $\hat{\tau}^{\text{ow}}$ with the overlap weight estimator. Under the homogeneity assumption, we impute all $Y_i(0)$ for the group $Z_i = 1$ by $Y_i - \hat{\tau}^{\text{ow}}$ and all $Y_i(1)$ for the group $Z_i = 0$ by $Y_i + \hat{\tau}^{\text{ow}}$. Then, we compute the pooled variance $S^2 = \mathbb{V}[Y(0)]$, correlation $\rho = \text{cor}(Y(0), W_e)$, and R-squared statistic $R^2 = \mathbb{V}[f(X)] / \mathbb{V}[Y(0)]$ empirically. Although τ_i varies individually, this homogeneous imputation ensures empirical S^2 , ρ , and R^2 calculated with imputed $Y(z)$ are the same for $z = 0, 1$ in the superpopulation. The (r, ϕ) remains unchanged from Section 5.1. Similarly, we use (r, ϕ, ρ^2) and the standardized effect $\tilde{\tau} = 1/S$ to calculate the required sample size N_{pos} and estimate the empirical power through $B = 10,000$ replications. The empirical power is the proportion of rejecting the null hypothesis in test (4) at level $\alpha = 0.05$ with the Hájek estimator over B replications. We report the simulation results in Table 2. We also conduct simulations using the same simulated superpopulations under ATT and ATO estimands, and results are relegated to Appendix C.3.

Table 2 reports the calculated sample sizes and empirical power under HTE. Remark 1 notes that under HTE, the asymptotic variance of the Hájek estimator additionally depends on $\mathbb{V}[\tau(X)]$, which is generally unavailable at the design stage. Nevertheless, the proposed method continues to achieve empirical power close to the nominal 0.80 across almost all overlap levels and both HTE scenarios, even when $\mathbb{V}(\tau_i)$ equals the true ATE. Similar to the case of homogeneous effect, the power with estimated propensity scores exceeds, often by a sizeable margin, that with the true scores under HTE. The comparison with the z -test and the method of Shook-Sa and Hudgens (2022) mirrors the homogeneous case: the z -test increasingly underestimates the required sample size as overlap deteriorates, while the SH method tracks the proposed method closely when ρ^2 is small, consistent with Remark 3.

5.3 Real-data-based nonparametric simulations

This section illustrates the proposed methods using simulations based on a widely used benchmark data from the Right Heart Catheterization (RHC) observational study (Connors et al., 1996), which was conducted to evaluate the causal effect of the diagnostic cardiological procedure of RHC (binary treatment) among hospitalized critically ill patients. The purpose of our simulation is not to re-design an existing study or conduct a *post-hoc* power analysis; instead, we want to assess the performance of the proposed methods in a real world setting where we do not know the true data generating model, presenting a more realistic and challenging setting. The data contain 5735 patients, each with 51 covariates (20 continuous, 25 binary, 6 categorical). The outcome is the binary survival status at 30 days after admission, with $Y = 1$ meaning death. In total, 2184 (38.1%) of the patients received the treatment and the rest did not. The death rate is 38.0% and 30.6% in the treatment and control group, respectively.

The simulation is outlined as follows. First, we calculate the summary parameters (r, ϕ, ρ^2) and the effect size $\tilde{\tau}^{\text{ATE}}$ from the real data. Second, we take these values as the only inputs of a hypothetical power analysis for a new observational study with the same goal on a similar population. We apply the proposed formula in Theorem 2 with these inputs to compute the minimal sample size N needed to achieve a certain level of power in detecting the pre-fixed effect size $\tilde{\tau}^{\text{ATE}}$. Third, we reverse the process to estimate the power using repeated bootstrapping samples of size N randomly drawn from the RHC data. The closer the estimated power is to the nominal power (e.g. 0.8), the more accurate our method is. This simulation is nonparametric because we do not assume any outcome model.

Following the above outline, from the real data we estimate the propensity scores using a logistic model with the main effects of each covariate. Based on these estimated scores, we numerically compute the true overlap coefficient ϕ defined in (9) to be 0.835. We also used the proposed normal approximation in Section 3.2, $W_e \sim \mathcal{N}(-0.701, 2.189)$, and estimate the overlap coefficient to be 0.822, which is close to the true value, showing the precision of our proposed Beta approximation. The Hájek estimate of the standardized effect size $\tilde{\tau}^{\text{ATE}}$ is 0.14. The treatment proportion is $r = 0.381$ and $\rho^2 = 0.000$. With these inputs alone, we apply formula (14) to calculate the minimal sample size to achieve 0.8 power to be 3625. We then reverse the process to calculate the actual power under a sample of 3625 units. Specifically, we generate $B = 1000$ replicates, each with 3625 rows randomly drawn from the original data with replacement. We calculate the Hájek estimate of τ^{ATE} and the associated 95% confidence interval in each replicate. Among the 1000 replicates, 924 intervals do not cover zero, giving an estimated power of 0.924 with 95% confidence interval (0.908 – 0.940), which is larger than the nominal power of 0.8. Potential reasons for the discrepancy include: (i) we used the estimated instead of the true propensity scores, and (ii) we treated the binary outcome as Gaussian. We also computed the sample size calculated by the two-sample z -test, which is 1567, leading to

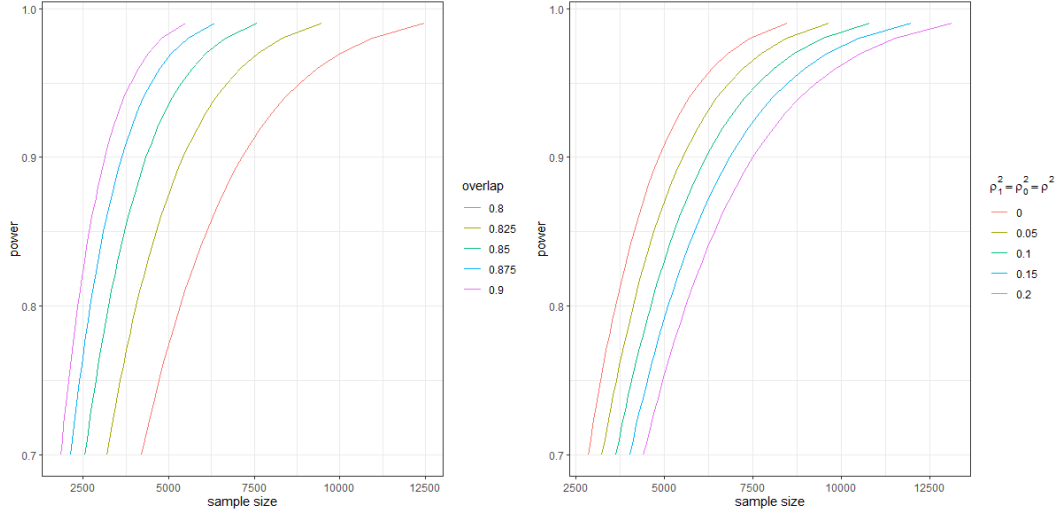


Figure 4: Power and sample size curves of an emulated Right Heart Catheterization study with an effect size $\tilde{\tau} = 0.14$ under different overlap coefficient ϕ (left) and the correlation $\rho = \rho_1 = \rho_0$ (right).

a vastly underpowered estimate with the power of only 0.55. Given that any real study would have data attrition due to missing data and extreme weights, a conservative (overpowered) estimate of the sample size is arguably more desirable than the opposite.

Figure 4 shows the power curves of τ^{ATE} given different values of the overlap coefficient ϕ and the correlation ρ^2 while fixing other summary inputs as those calculated from the RHC data. It shows that, to achieve the same power, the minimal sample size would increase as either the overlap ϕ decreases or the correlation ρ increases, matching the theoretical result in Corollary 1. The R^2 value is 0.21, which serves as the upper bound of ρ^2 .

We repeat the process for the ATO and ATT estimand, respectively, and the results suggest the proposed formula lead to reliable power calculation in a wide range of scenarios. Details are relegated to Appendix C.4.

6 Discussion

This paper establishes the theoretical foundation of power analysis for causal inference with observational data. We show that, compared with the power calculation of randomized trials, users only need to specify two additional parameters for emulated trials: an overlap coefficient ϕ that quantify the confounder-treatment association and a correlation parameter ρ that quantify the confounder-outcome association. We propose interpretable and easily computable statistics to characterize these two parameters. Our method requires a logistic model for the propensity scores and a homoscedastic restricted mean outcome model with a homogeneous treatment effect, but it bypasses distributional assumptions on the multivariate covariates due to the Lyapunov-type central limit theorem. In practice, investigators can set these parameters based on a pilot study or similar previous studies, or conduct related sensitivity analysis based on domain knowledge of these parameters.

A power analysis must be conducted before data collection. Once a study is carried out, it is generally not meaningful and in fact is misleading to perform a *post-hoc* power analysis on the collected data, e.g. using

the bootstrapping procedure in the RHC simulation in Section 5.3. Such a type of simulation cannot capture all the uncertainties in the causal effect because of the conditioning on the observed sample. Moreover, the observed data may not satisfy the model assumptions (e.g. effect homogeneity) underlying the sample size formula that the *post-hoc* power analysis implicitly assumes.

Some authors (e.g. Hernán, 2022) questioned the role of power analysis in observational studies; they argued that the primary consideration in observational studies is to reduce confounding bias rather than to achieve sufficient power. We agree on the central role of de-confounding in causal inference, but that does not preclude the critical role of power analysis in designing observational studies, which are usually subject to cost and time constraints. For example, in prospective studies of rare or severe diseases, recruiting patients is time-consuming, and thus investigators must determine the minimal sample size to achieve a reliable estimate before conducting the study. In this type of cohort studies, ideally investigators could recruit participants in batches, with the first batch serving as a pilot study, which provides reliable estimate of the key inputs (ϕ, ρ) and enables a more accurate calculation of the sample size needed for the subsequent batches. Another example concerns retrospective commercial population health data (such as the Truveta electronic health record data or IBM's MarketScan health insurance claims data), which usually charge users costs proportional to the data size and computational load. With limited resources, a sample size calculation is crucial for designing studies based on such data sources. Moreover, the same data source (e.g. disease registries or electronic health records of a population) are often used for investigating multiple hypotheses, e.g. effects on secondary outcomes in clinical research. In these cases, power analysis can help researchers decide how aggressive they can be with multiplicity correction or if they have to whittle down the primary objective.

There are several extensions of the proposed method in observational studies, including repeated outcomes, time-to-event outcomes, and multiple treatments. Propensity score weighting estimators for causal effects are available in all these settings. Therefore, we can readily adapt the general structure of power calculation developed in this paper. For example, for studies with repeated outcomes, a common estimand is the time-averaged difference; we can analyse the variance of an inverse probability weighted marginal outcome model within-subject correlation between outcomes. For time-to-event outcomes, a common estimand is the marginal causal hazard ratio from the Cox proportional hazard model; we can analyse the variance of the inverse probability weighted Cox model. Then, we can use the Beta approximation of the propensity score distribution to derive a closed-form expression of the variance inflation factor of the weighting estimator between an emulated trial and the corresponding randomized trial (Kish, 1965).

Acknowledgements

The authors thank the associate editor, three anonymous reviewers, Xiaoxiao Zhou, Jay Lusk, and Laine Thomas for constructive comments. This paper is dedicated to the memory of the late Sayan Mukherjee, who taught FL basics of power analysis and beyond.

References

- Abramowitz, M. and Stegun, I. A. (1965). *Handbook of Mathematical Functions with Formulas, Graphs, and Mathematical Tables*, volume 55. Dover, New York.
- Aitchison, J. and Shen, S. M. (1980). Logistic-normal distributions: Some properties and uses. *Biometrika*, 67(2):261–272.

- Bentkus, V. (2005). A Lyapunov-type bound in rd. *Theory of Probability & Its Applications*, 49(2):311–323.
- Bhattacharyya, A. (1943). On a measure of divergence between two statistical populations defined by their probability distribution. *Bulletin of the Calcutta Mathematical Society*, 35:99–110.
- Billingsley, P. (1995). *Probability and measure*. John Wiley & Sons.
- Branson, Z. and Dasgupta, T. (2020). Sampling-based randomised designs for causal inference under the potential outcomes framework. *International Statistical Review*, 88(1):101–121.
- Branson, Z., Li, X., and Ding, P. (2024). Power and sample size calculations for rerandomization. *Biometrika*, 111(1):355–363.
- Chow, S.-C., Shao, J., Wang, H., and Lokhnygina, Y. (2017). *Sample size calculations in clinical research*. Chapman and Hall/CRC.
- Connors, A. F., Speroff, T., Dawson, N. V., Thomas, C., Harrell, F. E., Wagner, D., Desbiens, N., Goldman, L., Wu, A. W., Califf, R. M., Fulkerson, W. J., Vidaillet, H., Broste, S., Bellamy, P., Lynn, J., and Knaus, W. A. (1996). The effectiveness of right heart catheterization in the initial care of critically ill patients. *Journal of the American Medical Association*, 276(11):889–897.
- Ding, P., Feller, A., and Miratrix, L. (2015). Randomization inference for treatment effect variation. *Journal of the Royal Statistical Society Series B: Statistical Methodology*, 78(3):655–671.
- Ding, P., Feller, A., and Miratrix, L. (2019). Decomposing treatment effect variation. *Journal of the American Statistical Association*, 114(525):304–317.
- Ding, P. and VanderWeele, T. J. (2016). Sensitivity analysis without assumptions. *Epidemiology*, 27(3):368–377.
- Hernán, M. A. (2022). Causal analyses of existing databases: no power calculations required. *Journal of clinical epidemiology*, 144:203–205.
- Hsieh, F. and Lavori, P. W. (2000). Sample-size calculations for the Cox proportional hazards regression model with nonbinary covariates. *Controlled clinical trials*, 21(6):552–560.
- Inman, H. F. and Bradley, E. L. (1989). The overlapping coefficient as a measure of agreement between probability distributions and point estimation of the overlap of two normal densities. *Communications in Statistics - Theory and Methods*, 18(10):3851–3874.
- Kelcey, B., Dong, N., Spybrook, J., and Cox, K. (2017). Statistical power for causally defined indirect effects in group-randomized trials with individual-level mediators. *Journal of Educational and Behavioral Statistics*, 42(5):499–530.
- Kish, L. (1965). *Survey sampling*. Wiley.
- Li, F., Morgan, K. L., and Zaslavsky, A. M. (2018a). Balancing covariates via propensity score weighting. *Journal of the American Statistical Association*, 113(521):390–400.
- Li, F., Thomas, L. E., and Li, F. (2019). Addressing extreme propensity scores via the overlap weights. *American journal of epidemiology*, 188(1):250–257.

- Li, F., Zaslavsky, A. M., and Landrum, M. B. (2013). Propensity score weighting with multilevel data. *Statistics in medicine*, 32(19):3373–3387.
- Li, X., Ding, P., and Rubin, D. B. (2018b). Asymptotic theory of rerandomization in treatment–control experiments. *Proceedings of the National Academy of Sciences*, 115(37):9157–9162.
- Lunceford, J. K. and Davidian, M. (2004). Stratification and weighting via the propensity score in estimation of causal treatment effects: a comparative study. *Statistics in medicine*, 23(19):2937–2960.
- Mukherjee, S., Tamayo, P., Rogers, S., Rifkin, R., Engle, A., Campbell, C., Golub, T. R., and Mesirov, J. P. (2003). Estimating dataset size requirements for classifying dna microarray data. *Journal of computational biology*, 10(2):119–142.
- Qin, X. (2024). Sample size and power calculations for causal mediation analysis: a tutorial and shiny app. *Behavior Research Methods*, 56(3):1738–1769.
- Raudenbush, S. W. (1997). Statistical analysis and optimal design for cluster randomised trials. *Psychological Methods*, 2(2):173–185.
- Rosenbaum, P. R. and Rubin, D. B. (1983). The central role of the propensity score in observational studies for causal effects. *Biometrika*, 70(1):41–55.
- Rubin, D. B. (1980). Randomization analysis of experimental data: The fisher randomization test comment. *Journal of the American Statistical Association*, 75(371):591–593.
- Shook-Sa, B. E. and Hudgens, M. G. (2022). Power and sample size for observational studies of point exposure effects. *Biometrics*, 78(1):388–398.
- Wendel, J. G. (1948). Note on the gamma function. *American Mathematical Monthly*, 55(9):563–564.
- Wooldridge, J. M. (2010). *Econometric Analysis of Cross Section and Panel Data*. The MIT Press.
- Yang, S. and Ding, P. (2018). Asymptotic inference of causal effects with observational studies trimmed by the estimated propensity scores. *Biometrika*, 105(2):487–493.
- Zeng, S., Li, F., Wang, R., and Li, F. (2021). Propensity score weighting for covariate adjustment in randomized clinical trials. *Statistics in medicine*, 40(4):842–858.

Appendix

A Proof of Propositions and Theorems

A.1 Proof of Equation (5)

Rewrite $\hat{\tau}_N = \tau + \epsilon\sqrt{V_0/N}$, where $\epsilon \sim \mathbf{N}(0, 1)$. Then the power of test is given by

$$\Pr\left(\tau + \epsilon\sqrt{\frac{V_0}{N}} > z_{1-\alpha}\sqrt{\frac{V}{N}}\right) = \Pr\left(\epsilon > z_{1-\alpha}\sqrt{\frac{V}{V_0}} - \tau\sqrt{\frac{N}{V_0}}\right) \quad (21)$$

$$= 1 - \Phi\left(\frac{z_{1-\alpha}\sqrt{V} - \tau\sqrt{N}}{\sqrt{V_0}}\right). \quad (22)$$

Equalizing this power with β , we obtain the sample size formula

$$N = \frac{\left(z_{1-\alpha}\sqrt{V} - z_{1-\beta}\sqrt{V_0}\right)^2}{\tau^2}. \quad (23)$$

Furthermore, when $\alpha < 0.5 < \beta$, $z_{1-\alpha} > 0$, $z_{1-\beta} < 0$, and hence we have

$$N \leq \frac{V}{\tau^2} (z_{1-\alpha} - z_{1-\beta})^2 = \frac{V}{\tau^2} (z_{1-\alpha} + z_\beta)^2. \quad (24)$$

A.2 Special case of the Lyapunov Central Limit Theorem

For completeness, we first present the general form of the Lyapunov Central Limit Theorem (CLT).

Theorem 3 (Lyapunov CLT). *Suppose $\{Z_1, \dots, Z_n, \dots\}$ is a sequence of independent random variables, each with finite expected value μ_i and variance σ_i^2 . Define $s_n^2 = \sum_{i=1}^n \sigma_i^2$. If for some $\delta > 0$, the Lyapunov's condition*

$$\lim_{n \rightarrow \infty} \frac{1}{s_n^{2+\delta}} \sum_{i=1}^n \mathbb{E}[|Z_i - \mu_i|^{2+\delta}] = 0 \quad (25)$$

is satisfied, then

$$\frac{1}{s_n} \sum_{i=1}^n (Z_i - \mu_i) \Rightarrow \mathbf{N}(0, 1). \quad (26)$$

As a special case, let $Z_i = \beta_i X_i$, where $\{X_1, \dots, X_n, \dots\}$ is a sequence of independent random variables with expectation 0 and variance 1. Then Z_i has expectation 0 and variance β_i^2 . Assume (1) $\mathbb{E}[X_i^4] \leq B < \infty$ and (2) $M_n \equiv \frac{\max_{1 \leq i \leq n} \beta_i^2}{\sum_{i=1}^n \beta_i^2} = o(1)$, then the Lyapunov's condition is satisfied (by taking $\delta = 2$) because

$$\begin{aligned} \lim_{n \rightarrow \infty} \frac{1}{\left(\sum_{i=1}^n \beta_i^2\right)^2} \sum_{i=1}^n \beta_i^4 \mathbb{E}[X_i^4] &\leq B \lim_{n \rightarrow \infty} \frac{\sum_{i=1}^n \beta_i^4}{\left(\sum_{i=1}^n \beta_i^2\right)^2} \\ &\leq B \lim_{n \rightarrow \infty} \frac{\max_{1 \leq i \leq n} \beta_i^2 \sum_{i=1}^n \beta_i^2}{\left(\sum_{i=1}^n \beta_i^2\right)^2} \\ &= B \lim_{n \rightarrow \infty} M_n \\ &= 0. \end{aligned}$$

Therefore, $\sum_{i=1}^n \beta_i X_i$ is approximately a normal distribution with mean 0 and variance $\sum_{i=1}^n \beta_i^2$ when n is large.

A.3 Proof of Proposition 1(i)

Suppose $U \sim \text{Beta}(a, b)$ and $Z \sim \text{Bin}(U)$. Then,

$$\mathbb{E}[Z] = \mathbb{E}[\mathbb{E}[Z | U]] = \mathbb{E}[U] = \frac{a}{a+b}. \quad (27)$$

Furthermore, define $f_z(u) = \Pr(U = u | Z = z)$ for $z \in \{0, 1\}$. By Bayes' rule,

$$f_z(u) = \Pr(U = u | Z = z) = \frac{\Pr(U = u) \Pr(Z = z | U = u)}{\Pr(Z = z)}. \quad (28)$$

Therefore,

$$\begin{aligned} f_1(u) &= \frac{\Pr(U = u)u}{a/(a+b)} = \frac{\Gamma(a+b)}{\Gamma(a)\Gamma(b)} \frac{u^a(1-u)^{b-1}}{a/(a+b)} = \frac{\Gamma(a+b+1)}{\Gamma(a+1)\Gamma(b)} u^a(1-u)^{b-1}, \\ f_0(u) &= \frac{\Pr(U = u)(1-u)}{b/(a+b)} = \frac{\Gamma(a+b)}{\Gamma(a)\Gamma(b)} \frac{u^{a-1}(1-u)^b}{b/(a+b)} = \frac{\Gamma(a+b+1)}{\Gamma(a)\Gamma(b+1)} u^{a-1}(1-u)^b. \end{aligned}$$

Consequently,

$$\begin{aligned} \phi &= \int_0^1 \sqrt{\frac{\Gamma(a+b+1)^2}{\Gamma(a+1)\Gamma(b)\Gamma(a)\Gamma(b+1)}} u^{a-0.5}(1-u)^{b-0.5} du \\ &= \frac{\Gamma(a+b+1)}{\sqrt{a}\Gamma(a)\sqrt{b}\Gamma(b)} \cdot \frac{\Gamma(a+0.5)\Gamma(b+0.5)}{\Gamma(a+b+1)} \\ &= \frac{\Gamma(a+0.5)}{\sqrt{a}\Gamma(a)} \frac{\Gamma(b+0.5)}{\sqrt{b}\Gamma(b)}. \end{aligned}$$

A.4 Proof of Proposition 1(ii)

Denote ϕ by $\phi(a, b)$ to indicate that ϕ is a function of a and b , and factorize it as $\phi(a, b) = \tilde{\phi}(a)\tilde{\phi}(b)$, where $\tilde{\phi}(x) = \Gamma(x+0.5)/\{\sqrt{x}\Gamma(x)\}$.

To show $\phi(a, b)$ increases monotonically in a (and b), it suffices to show that the partial derivative of $\log \phi(a, b) = \log \tilde{\phi}(a) + \log \tilde{\phi}(b)$ with respect to a (and b) is positive. By seeing that $\log \tilde{\phi}(x) = \log \Gamma(x+0.5) - \log \Gamma(x) - \log \sqrt{x}$, we have

$$\frac{\partial \log \phi(a, b)}{\partial a} = \frac{d \log \tilde{\phi}(a)}{da} = \psi(a + \frac{1}{2}) - \psi(a) - \frac{1}{2a}, \quad (29)$$

where $\psi(x) = d \log \Gamma(x)/dx$ is the digamma function.

Leveraging Abramowitz and Stegun (1965) Equation (6.3.22), we have

$$\psi(x) - \psi(y) = \int_0^1 \frac{t^{y-1} - t^{x-1}}{1-t} dt, \quad \forall x, y > 0. \quad (30)$$

Plugging into Equation (29) yields

$$\psi(a + \frac{1}{2}) - \psi(a) = \int_0^1 \frac{t^{a-1} - t^{a-1/2}}{1-t} dt = \int_0^1 \frac{t^{a-1}}{1+\sqrt{t}} dt > \int_0^1 \frac{t^{a-1}}{2} dt = \frac{1}{2a}, \quad (31)$$

which leads to

$$\frac{\partial \log \phi(a, b)}{\partial a} > 0. \quad (32)$$

Therefore, $\log \phi(a, b)$ increases monotonically in a and so does $\phi(a, b)$. By symmetry, $\phi(a, b)$ also increases monotonically in b .

A.5 Proof of Proposition 1(iii)

To see the 1-1 mapping between $(r, \phi) \in (0, 1)^2$ and $(a, b) \in (0, +\infty)^2$, it suffices to provide an injective and surjective mapping from (a, b) to (r, ϕ) . Define the mapping $h : (a, b) \rightarrow (r, \phi)$ as

$$h : (a, b) \rightarrow \left(r = \frac{a}{a+b}, \phi = \tilde{\phi}(a)\tilde{\phi}(b) \right), \quad (33)$$

where $\tilde{\phi}(x)$ is defined in Appendix A.4.

Before showing that h is injective and surjective, we first establish the properties of the restricted univariate mapping from a to ϕ for arbitrarily fixed $r \in (0, 1)$ induced by h , denoted as $\phi_h(a; r)$. For fixed r , we have $b = a(1-r)/r$, and h maps (a, b) to $(r, \phi_h(a; r))$, where $\phi_h(a; r)$ is defined as

$$\phi_h(a; r) = \tilde{\phi}(a)\tilde{\phi}(b) = \tilde{\phi}(a)\tilde{\phi}(a(1-r)/r). \quad (34)$$

First, $\phi_h(a; r)$ increases monotonically in a , because

$$\frac{d \log \phi_h(a; r)}{da} = \frac{d \log \tilde{\phi}(a)}{da} + \frac{d \log \tilde{\phi}(b)}{da} = \frac{d \log \tilde{\phi}(a)}{da} + \frac{d \log \tilde{\phi}(b)}{db} \frac{db}{da} > 0, \quad (35)$$

by Equation (29), Equation (32), and $db/da = (1-r)/r > 0$.

Second, the image of $\phi_h(a; r)$ is $(0, 1)$, i.e., $\phi_h(a; r)$ maps $a \in (0, +\infty)$ onto the domain of ϕ excluding 0 and 1. Evaluate the limit of $\tilde{\phi}(x)$ at $x \rightarrow 0^+$ and $x \rightarrow +\infty$ respectively, we have

$$\lim_{x \rightarrow 0^+} \tilde{\phi}(x) = \lim_{x \rightarrow 0^+} \frac{\Gamma(x+0.5)}{\sqrt{x}\Gamma(x)} = \lim_{x \rightarrow 0^+} \sqrt{x} \frac{\Gamma(x+0.5)}{\Gamma(x+1)} = 0 \times \frac{\sqrt{\pi}}{1} = 0, \quad (36)$$

by using $\Gamma(x) = \Gamma(x+1)/x$, and

$$\lim_{x \rightarrow +\infty} \tilde{\phi}(x) = \lim_{x \rightarrow +\infty} \frac{\Gamma(x+0.5)}{\sqrt{x}\Gamma(x)} = 1, \quad (37)$$

by Equation (12) in Wendel (1948). Since both limits are finite and $a \rightarrow 0^+$ (or $+\infty$) implies $b \rightarrow 0^+$ (or $+\infty$) respectively, therefore

$$\lim_{a \rightarrow 0^+} \phi_h(a; r) = 0, \quad \lim_{a \rightarrow +\infty} \phi_h(a; r) = 1. \quad (38)$$

Given that $\phi_h(a; r)$ is continuous and monotonically increasing in a , by intermediate value theorem, for any $\phi^* \in (0, 1)$ there exists a unique a^* such that $\phi_h(a^*; r) = \phi^*$. Therefore, the image of $\phi_h(a; r)$ is $(0, 1)$.

Now, we show h is injective and surjective. For injectivity, suppose that h maps (a_1, b_1) and (a_2, b_2) to

the same (r, ϕ) . Therefore, $\phi_h(a_1; r) = \phi_h(a_2; r) = \phi$. Since $\phi_h(a; r)$ is monotonic in a , so $a_1 = a_2$, hence $b_1 = a_1(1-r)/r = a_2(1-r)/r = b_2$, establishing injectivity.

For surjectivity, pick an arbitrary $(r^*, \phi^*) \in (0, 1)^2$. It induces $\phi_h(a; r^*)$ which has the image of $(0, 1)$, so there exists a^* such that $\phi_h(a^*; r^*) = \phi^*$. Define $b^* = a^*(1-r^*)/r^*$, then h maps (a^*, b^*) to (r^*, ϕ^*) , establishing surjectivity.

A.6 Proof of Equation (12)

Recall $e(X) = \text{expit}(W_e)$ and $W_e \sim \mathcal{N}(\mu_e, \sigma_e^2)$ given in Section 3.2, and $Y(z) = aW_e + z\tau + \epsilon$ given in Section 3.3, where ϵ is the compound error and $\mathbb{E}[\epsilon] = \mu$ and $\mathbb{V}[\epsilon] = \sigma_y^2$. For clarity of the proof, we write out $\epsilon = W_e^\perp + \epsilon_{ori}$, where ϵ_{ori} is the original error term defined in the RMM Model (11).

By the definition of Model (11), ϵ_{ori} is uncorrelated with any measurable function of X , including W_e , and therefore $\text{Cov}(W_e, \epsilon) = \text{Cov}(W_e, W_e^\perp) + \text{Cov}(W_e, \epsilon_{ori}) = 0$. Hence we have the following results:

$$S^2 \equiv \mathbb{V}[Y(0)] = \mathbb{V}[aW_e + \epsilon] = a^2\sigma_e^2 + \sigma_y^2; \quad (39)$$

$$\rho \equiv \text{cor}[Y(0), W_e] = \text{cor}[aW_e + \epsilon, W_e] = a\sqrt{\sigma_e^2/S^2}. \quad (40)$$

By (40), $a = \rho\sqrt{S^2/\sigma_e^2}$, which, plugged into (39), yields

$$\sigma_y^2 = (1 - \rho^2)S^2. \quad (41)$$

A.7 Proof of the analytical form of variance V in Theorem 2

Recall that

$$V = \mathbb{E} \left[\frac{\{Y(1) - \mathbb{E}[Y(1)]\}^2}{e(X)} \right] + \mathbb{E} \left[\frac{\{Y(0) - \mathbb{E}[Y(0)]\}^2}{1 - e(X)} \right], \quad (42)$$

where $e(X)$ and $Y(z)$ are given in Appendix A.6. We first state all necessary results regarding ϵ , ϵ_{ori} , W_e , and W_e^\perp in Lemma 4.

Lemma 4. *Under the joint Gaussianity of $(f(X), W_e)$ and the RMM Model 11:*

- (1) $\mathbb{E}[\epsilon_{ori}|W_e] = 0$
- (2) $\mu = \mathbb{E}[\epsilon] = \mathbb{E}[\epsilon|W_e] = \mathbb{E}[W_e^\perp]$
- (3) $\mathbb{E}[\epsilon_{ori}|W_e, W_e^\perp] = 0$
- (4) $\text{Cov}(W_e^\perp, \epsilon_{ori}) = 0$

Lemma 4 holds because: (1) $\mathbb{E}[\epsilon_{ori}|X] = 0$ and the law of iterated expectation, see Section 2.2.4 of Wooldridge (2010), that $\mathbb{E}[\epsilon_{ori}|W_e] = \mathbb{E}\{\mathbb{E}[\epsilon_{ori}|X] | W_e\} = 0$. (2) W_e and W_e^\perp are independent, and $\mathbb{E}[\epsilon|W_e] = \mathbb{E}[W_e^\perp|W_e] + \mathbb{E}[\epsilon_{ori}|W_e] = \mathbb{E}[W_e^\perp]$. (3) $\mathbb{E}[\epsilon_{ori}|W_e, W_e^\perp] = \mathbb{E}[\epsilon_{ori}|W_e, f(X)] = \mathbb{E}\{\mathbb{E}[\epsilon_{ori}|X] | W_e, f(X)\} = 0$, see that any one of $(f(X), W_e, W_e^\perp)$ is determined by another two. (4) $W_e^\perp = f(X) - aW_e$ is a function of X and therefore uncorrelated with ϵ_{ori} by the definition of RMM.

We derive the first term in V , and similar result holds for the second term by symmetry.

$$\mathbb{E} \left[\frac{\{Y(1) - \mathbb{E}[Y(1)]\}^2}{e(X)} \right] = \mathbb{E} \left[\frac{\{a(W_e - \mu_e) + (\epsilon - \mu)\}^2}{\text{expit}(W_e)} \right] \quad (43)$$

$$= a^2 \mathbb{E} \left[\frac{(W_e - \mu_e)^2}{\text{expit}(W_e)} \right] + \mathbb{E} \left[\frac{(\epsilon - \mu)^2}{\text{expit}(W_e)} \right] + 2a \mathbb{E} \left[\frac{(W_e - \mu_e)(\epsilon - \mu)}{\text{expit}(W_e)} \right] \quad (44)$$

$$:= A + B + C \quad (45)$$

Term A only depends on the propensity score model but not the outcome model, while B and C involve both models. We first derive B and C .

$$B = \mathbb{E} \left\{ \mathbb{E} \left[\frac{(\epsilon - \mu)^2}{\text{expit}(W_e)} \middle| W_e \right] \right\} = \mathbb{E} \left\{ \frac{\mathbb{E}[(\epsilon - \mu)^2 | W_e]}{\text{expit}(W_e)} \right\} = \mathbb{E} \left\{ \frac{\mathbb{V}[\epsilon | W_e]}{\text{expit}(W_e)} \right\}, \quad (46)$$

and for $\mathbb{V}[\epsilon | W_e]$ we have

$$\mathbb{V}[\epsilon | W_e] = \mathbb{V}[W_e^\perp | W_e] + \mathbb{V}[\epsilon_{ori} | W_e] + 2 \text{Cov}(W_e^\perp, \epsilon_{ori} | W_e). \quad (47)$$

For these three pieces: $\mathbb{V}[W_e^\perp | W_e] = \mathbb{V}[W_e^\perp]$ because W_e is independent of W_e^\perp ; $\mathbb{V}[\epsilon_{ori} | W_e] = \mathbb{V}[\epsilon_{ori}]$ because of the homoskedasticity assumption that $\mathbb{V}[\epsilon_{ori} | e(X)] = \mathbb{V}[\epsilon_{ori}]$, and W_e is a deterministic function of $e(X)$; and for the last piece,

$$\text{Cov}(W_e^\perp, \epsilon_{ori} | W_e) = \mathbb{E}[W_e^\perp \cdot \epsilon_{ori} | W_e] - \mathbb{E}[W_e^\perp | W_e] \mathbb{E}[\epsilon_{ori} | W_e] \quad (48)$$

$$= \mathbb{E} \left\{ W_e^\perp \cdot \mathbb{E}[\epsilon_{ori} | W_e, W_e^\perp] \middle| W_e \right\} - 0, \quad \text{by Lemma 4 (1)} \quad (49)$$

$$= \mathbb{E} \left\{ W_e^\perp \cdot 0 \middle| W_e \right\} = 0, \quad \text{by Lemma 4 (3)}. \quad (50)$$

Therefore, $\mathbb{V}[\epsilon | W_e]$ is invariant to W_e by seeing that

$$\mathbb{V}[\epsilon | W_e] = \mathbb{V}[W_e^\perp] + \mathbb{V}[\epsilon_{ori}] + 0 = \mathbb{V}[\epsilon] = \sigma_y^2, \quad (51)$$

and consequently

$$B = \mathbb{E} \left\{ \frac{\mathbb{V}[\epsilon | W_e]}{\text{expit}(W_e)} \right\} = \sigma_y^2 \cdot \mathbb{E} \left[\frac{1}{\text{expit}(W_e)} \right] \quad (52)$$

Finally, for C ,

$$C = 2a \cdot \mathbb{E} \left\{ \frac{W_e - \mu_e}{\text{expit}(W_e)} \mathbb{E}[\epsilon - \mu | W_e] \right\} \quad (53)$$

$$= 2a \cdot \mathbb{E} \left\{ \frac{W_e - \mu_e}{\text{expit}(W_e)} (\mathbb{E}[\epsilon | W_e] - \mathbb{E}[W_e^\perp]) \right\}, \quad \text{by Lemma 4 (2)} \quad (54)$$

$$= 2a \cdot \mathbb{E} \left\{ \frac{W_e - \mu_e}{\text{expit}(W_e)} \cdot 0 \right\} = 0. \quad (55)$$

Gathering A , B , and C above,

$$\mathbb{E} \left[\frac{\{Y(1) - \mathbb{E}[Y(1)]\}^2}{e(X)} \right] = a^2 \cdot \mathbb{E} \left[\frac{(W_e - \mu_e)^2}{\text{expit}(W_e)} \right] + \sigma_y^2 \cdot \mathbb{E} \left[\frac{1}{\text{expit}(W_e)} \right], \quad (56)$$

which is fully determined under a^2 , σ_y^2 , and the distribution of W_e , as calculated below.

$$\mathbb{E} \left[\frac{1}{\text{expit}(W_e)} \right] = \int (1 + e^{-w}) \frac{1}{\sqrt{2\pi\sigma_e^2}} \exp \left(-\frac{(w - \mu_e)^2}{2\sigma_e^2} \right) dw \quad (57)$$

$$= \int (1 + e^{-u - \mu_e}) \frac{1}{\sqrt{2\pi\sigma_e^2}} \exp \left(-\frac{u^2}{2\sigma_e^2} \right) du \quad (58)$$

$$= 1 + \exp \left(-\mu_e + \frac{1}{2}\sigma_e^2 \right), \quad (59)$$

$$\mathbb{E} \left[\frac{(W_e - \mu_e)^2}{\text{expit}(W_e)} \right] = \int (w - \mu_e)^2 (1 + e^{-w}) \frac{1}{\sqrt{2\pi\sigma_e^2}} \exp \left(-\frac{(w - \mu_e)^2}{2\sigma_e^2} \right) dw \quad (60)$$

$$= \int u^2 (1 + e^{-u - \mu_e}) \frac{1}{\sqrt{2\pi\sigma_e^2}} \exp \left(-\frac{u^2}{2\sigma_e^2} \right) du \quad (61)$$

$$= \sigma_e^2 + (\sigma_e^4 + \sigma_e^2) \exp \left(-\mu_e + \frac{1}{2}\sigma_e^2 \right). \quad (62)$$

Therefore,

$$\mathbb{E} \left[\frac{\{Y(1) - \mathbb{E}[Y(1)]\}^2}{e(X)} \right] = a^2\sigma_e^2 + \sigma_y^2 + [a^2\sigma_e^2(\sigma_e^2 + 1) + \sigma_y^2] \exp \left(-\mu_e + \frac{1}{2}\sigma_e^2 \right). \quad (63)$$

Similarly,

$$\mathbb{E} \left[\frac{\{Y(0) - \mathbb{E}[Y(0)]\}^2}{1 - e(X)} \right] = a^2\sigma_e^2 + \sigma_y^2 + [a^2\sigma_e^2(\sigma_e^2 + 1) + \sigma_y^2] \exp \left(\mu_e + \frac{1}{2}\sigma_e^2 \right). \quad (64)$$

Adding (63) and (64), we have

$$V = 2(a^2\sigma_e^2 + \sigma_y^2) + 2 [a^2\sigma_e^2(\sigma_e^2 + 1) + \sigma_y^2] \exp \left(\frac{\sigma_e^2}{2} \right) \cosh(\mu_e). \quad (65)$$

Plugging in the expression for a and σ_y^2 ,

$$V = 2S^2 \left\{ 1 + (\rho^2\sigma_e^2 + 1) \exp \left(\frac{\sigma_e^2}{2} \right) \cosh(\mu_e) \right\}. \quad (66)$$

A.8 Proof of the asymptotic variance of the general Hájek WATE estimator

Let

$$\xi_1^* = \frac{\mathbb{E}[h(X_i; \alpha^*)Y_i(1)]}{\mathbb{E}[h(X_i; \alpha^*)]}, \quad \xi_0^* = \frac{\mathbb{E}[h(X_i; \alpha^*)Y_i(0)]}{\mathbb{E}[h(X_i; \alpha^*)]}$$

be the expected potential outcomes given the tilting function $h(x)$ and let α^* be the true parameter value for the propensity score model $e(X; \alpha)$. Let

$$\hat{\xi}_1 = \frac{\sum_{i=1}^N Z_i Y_i \hat{w}_1(X_i)}{\sum_{i=1}^N Z_i \hat{w}_1(X_i)}, \quad \hat{\xi}_0 = \frac{\sum_{i=1}^N (1 - Z_i) Y_i \hat{w}_0(X_i)}{\sum_{i=1}^N (1 - Z_i) \hat{w}_0(X_i)},$$

and

$$\hat{\tau}_w = \hat{\xi}_1 - \hat{\xi}_0.$$

Then $(\hat{\xi}_1, \hat{\xi}_0, \hat{\alpha})$ jointly solves

$$0 = \frac{1}{N} \sum_{i=1}^N \phi(Y_i(1), Y_i(0), x_i, Z_i; \xi_1, \xi_0, \alpha) = \frac{1}{N} \sum_{i=1}^N \begin{pmatrix} \phi_1(Y_i(1), x_i, Z_i; \xi_1, \alpha) \\ \phi_0(Y_i(0), x_i, Z_i; \xi_0, \alpha) \\ \psi_\alpha(x_i, Z_i; \alpha) \end{pmatrix}$$

where

$$\phi = \begin{pmatrix} \phi_1 \\ \phi_0 \\ \psi_\alpha \end{pmatrix} \quad \text{with} \quad \begin{aligned} \phi_1 &= Z_i \cdot w_1(X_i; \alpha) \cdot \{Y_i(1) - \xi_1\}, \\ \phi_0 &= (1 - Z_i) \cdot w_0(X_i; \alpha) \cdot \{Y_i(0) - \xi_0\}, \\ \psi_\alpha &= e'(X_i; \alpha) \{Z_i - e(X_i; \alpha)\}. \end{aligned} \quad (67)$$

It is straightforward to verify that $\mathbb{E}[\phi(\xi_1^*, \xi_0^*, \alpha^*)] = 0$. The theory of M-estimation states that

$$\sqrt{N} \begin{pmatrix} \hat{\xi}_1 - \xi_1^* \\ \hat{\xi}_0 - \xi_0^* \\ \hat{\alpha} - \alpha^* \end{pmatrix} \xrightarrow{d} \mathcal{N}(0, (A^*)^{-1} B^* (A^*)^{-\top}), \quad (68)$$

where A^* and B^* are the values of $-\mathbb{E} \left(\frac{\partial \phi}{\partial (\xi_1, \xi_0, \alpha)} \right)$ and $\mathbb{E}[\phi \phi^\top]$ evaluated at $(\xi_1^*, \xi_0^*, \alpha^*)$ respectively.

Calculation of A^* .

By definition, we have

$$\frac{\partial \phi}{\partial (\xi_1, \xi_0, \alpha)} \Big|_{(\xi_1^*, \xi_0^*, \alpha^*)} = \begin{pmatrix} \frac{\partial \phi_1^*}{\partial \xi_1} & 0 & \frac{\partial \phi_1^*}{\partial \alpha} \\ 0 & \frac{\partial \phi_0^*}{\partial \xi_0} & \frac{\partial \phi_0^*}{\partial \alpha} \\ 0 & 0 & \frac{\partial \psi_\alpha^*}{\partial \alpha} \end{pmatrix} \quad (69)$$

where

$$\begin{aligned} \frac{\partial \phi_1^*}{\partial \xi_1} &= -Z_i \cdot w_1(X_i; \alpha^*), \\ \frac{\partial \phi_0^*}{\partial \xi_0} &= -(1 - Z_i) \cdot w_0(X_i; \alpha^*), \\ \frac{\partial \phi_1^*}{\partial \alpha} &= Z_i \cdot \{Y_i(1) - \xi_1^*\} \cdot w_1'(X_i; \alpha^*), \\ \frac{\partial \phi_0^*}{\partial \alpha} &= (1 - Z_i) \cdot \{Y_i(0) - \xi_0^*\} \cdot w_0'(X_i; \alpha^*), \\ \frac{\partial \psi_\alpha^*}{\partial \alpha} &= e''(X_i; \alpha^*) (Z_i - e(X_i; \alpha^*)) - [e'(X_i; \alpha^*)] [e'(X_i; \alpha^*)]^\top. \end{aligned}$$

Accordingly, we have

$$A^* = \begin{pmatrix} a_{11} & 0 & a_{13} \\ 0 & a_{22} & a_{23} \\ 0 & 0 & a_{33} \end{pmatrix},$$

where $a_{11} = \mathbb{E}[Z_i \cdot w_1(X_i; \alpha^*)] = \mathbb{E}[e(X_i; \alpha^*)w_1(X_i; \alpha^*)] = \mathbb{E}[h(X_i; \alpha^*)]$.

Calculation of B^* .

$$B^* = \mathbb{E}[\phi^* \phi^{*\top}] = \begin{pmatrix} b_{11} & 0 & b_{13} \\ 0 & b_{22} & b_{23} \\ b_{13}^\top & b_{23}^\top & b_{33} \end{pmatrix},$$

where

$$\begin{aligned} b_{11} &= \mathbb{E}[Z_i \cdot \{Y_i(1) - \xi_1^*\}^2 \cdot w_1(X_i; \alpha^*)^2] = \mathbb{E}[\{Y_i(1) - \xi_1^*\}^2 e(X_i; \alpha^*) w_1(X_i; \alpha^*)^2], \\ b_{22} &= \mathbb{E}[(1 - Z_i) \cdot \{Y_i(0) - \xi_0^*\}^2 \cdot w_0(X_i; \alpha^*)^2] \\ &= \mathbb{E}[\{Y_i(0) - \xi_0^*\}^2 \{1 - e(X_i; \alpha^*)\} w_0(X_i; \alpha^*)^2]. \end{aligned}$$

Calculation of $(A^*)^{-1}B^*(A^*)^{-\top}$.

First, we notice that

$$A^* = \begin{pmatrix} a_{11} & 0 & a_{13} \\ 0 & a_{11} & a_{23} \\ 0 & 0 & a_{33} \end{pmatrix} \implies (A^*)^{-1} = \begin{pmatrix} a_{11}^{-1} & 0 & -a_{11}^{-1}a_{13}a_{33}^{-1} \\ 0 & a_{11}^{-1} & -a_{11}^{-1}a_{23}a_{33}^{-1} \\ 0 & 0 & a_{33}^{-1} \end{pmatrix}$$

Therefore,

$$\begin{aligned} &(A^*)^{-1}B^*(A^*)^{-\top} \\ &= \begin{pmatrix} a_{11}^{-1} & 0 & -a_{11}^{-1}a_{13}a_{33}^{-1} \\ 0 & a_{11}^{-1} & -a_{11}^{-1}a_{23}a_{33}^{-1} \\ 0 & 0 & a_{33}^{-1} \end{pmatrix} \begin{pmatrix} b_{11} & 0 & b_{13} \\ 0 & b_{22} & b_{23} \\ b_{13}^\top & b_{23}^\top & b_{33} \end{pmatrix} \begin{pmatrix} a_{11}^{-1} & 0 & 0 \\ 0 & a_{11}^{-1} & 0 \\ -a_{33}^{-1}c_{13}^\top a_{11}^{-1} & -a_{33}^{-1}c_{23}^\top a_{11}^{-1} & a_{33}^{-1} \end{pmatrix} \\ &= a_{11}^{-2} \begin{pmatrix} b_{11} - 2a_{13}a_{33}^{-1}b_{13}^\top + a_{13}a_{33}^{-1}a_{13}^\top & -a_{13}a_{33}^{-1}b_{23}^\top - b_{13}a_{33}^{-1}a_{23}^\top + a_{13}a_{33}^{-1}a_{23}^\top & * \\ -a_{13}a_{33}^{-1}b_{23}^\top - b_{13}a_{33}^{-1}a_{23}^\top + a_{13}a_{33}^{-1}a_{23}^\top & b_{22} - 2a_{23}a_{33}^{-1}b_{23}^\top + a_{23}a_{33}^{-1}a_{23}^\top & * \\ * & * & * \end{pmatrix}. \end{aligned}$$

Hence,

$$\begin{aligned} \text{Var}(\hat{\tau}_w) &= \begin{pmatrix} 1 & -1 & 0 \end{pmatrix} (A^*)^{-1}B^*(A^*)^{-\top} \begin{pmatrix} 1 \\ -1 \\ 0 \end{pmatrix} \\ &= a_{11}^{-2} [(b_{11} + b_{22} - 2(a_{13} - a_{23})a_{33}^{-1}(b_{13} - b_{23})^\top + (a_{13} - a_{23})a_{33}^{-1}(a_{13} - a_{23})^\top)]. \end{aligned}$$

When the propensity scores are assumed known, $e'(X_i; \alpha^*) = 0$, and hence $a_{13} = a_{23} = 0$. Consequently, the variance reduces to $a_{11}^{-2}(b_{11} + b_{22})$. However, unlike ATE, there is no theoretical guarantee on whether assuming known propensity score leads to a larger or a smaller variance.

A.9 Proof of (19)

See Appendix 12 that $Y(z) = aW_e + z\tau + \epsilon$, where $\epsilon = W_e^\perp + \epsilon_{ori}$ is the compound error with $\mathbb{E}[\epsilon] = \mu$ and

$\mathbb{V}[\epsilon] = \sigma_y^2$. ϵ_{ori} is the error term defined in Model (11). Then,

$$\xi_z = \frac{\mathbb{E}[h(X)Y(z)]}{\mathbb{E}[h(X)]} = a \frac{\mathbb{E}[h(W_e)W_e]}{\mathbb{E}[h(W_e)]} + \frac{\mathbb{E}[h(W_e)z\tau]}{\mathbb{E}[h(W_e)]} + \frac{\mathbb{E}[h(W_e)\epsilon]}{\mathbb{E}[h(W_e)]} \quad (70)$$

$$= a \frac{\mathbb{E}[h(W_e)W_e]}{\mathbb{E}[h(W_e)]} + z\tau + \mu. \quad (71)$$

The last equation holds because of Lemma 4 (2). Then,

$$\begin{aligned} & \mathbb{E} \left[\frac{(Y_i(1) - \xi_1)^2}{e(X_i)} h(X_i)^2 \right] \\ &= \mathbb{E} \left[\left\{ a \left(W_e - \frac{\mathbb{E}[h(W_e)W_e]}{\mathbb{E}[h(W_e)]} \right) + \epsilon - \mu \right\}^2 \frac{h(W_e)^2}{\text{expit}(W_e)} \right] \end{aligned} \quad (72)$$

$$= \mathbb{E} \left[\mathbb{E} \left[\left\{ a \left(W_e - \frac{\mathbb{E}[h(W_e)W_e]}{\mathbb{E}[h(W_e)]} \right) + \epsilon - \mu \right\}^2 \frac{h(W_e)^2}{\text{expit}(W_e)} \mid W_e \right] \right] \quad (73)$$

$$= \mathbb{E} \left[\left\{ a^2 \left(W_e - \frac{\mathbb{E}[h(W_e)W_e]}{\mathbb{E}[h(W_e)]} \right)^2 + \sigma_y^2 \right\} \frac{h(W_e)^2}{\text{expit}(W_e)} \right] \quad (74)$$

$$= a^2 \mathbb{E} \left[\left(W_e - \frac{\mathbb{E}[h(W_e)W_e]}{\mathbb{E}[h(W_e)]} \right)^2 \frac{h(W_e)^2}{\text{expit}(W_e)} \right] + \sigma_y^2 \mathbb{E} \left[\frac{h(W_e)^2}{\text{expit}(W_e)} \right]. \quad (75)$$

The third equation holds because $\mathbb{V}[\epsilon|W_e] = \mathbb{V}[\epsilon]$ and the cross term equals zero, see Appendix A.7. Similar derivation yields the other equation on $Y_i(0)$.

B Examples

B.1 Empirical examples of normality of linear combination of covariates

We consider the simulated data in Section 5 and three real world datasets: (i) RHC; (ii) the Best Apnea Interventions for Research (BestAIR) trial, a individually randomized trial with 169 units, with 9 continuous or binary covariates; more details can be found in Zeng et al. (2021); (iii) HSR: an observational study on the racial disparities of breast cancer screening, with 56,480 units and 17 binary covariates; more details can be found in Li et al. (2013). For each dataset, we fit a simple logistic model to estimate the propensity score $e(X) = \text{expit}(\beta_0 + X'\beta)$, and we provide the density plot and Q-Q plot in Figure 5. Normality holds approximately in all the cases.

B.2 Examples of the Beta approximation of logit-normal distribution.

Figure 6 presents the density of the Beta distribution over a grid of (a, b) values within $\{0.5, 1, 2, 3\}$, and the density of the corresponding approximated logit-normal distributions.

B.3 Calculation of overlap coefficient ϕ with fitted propensity scores

In practice, researchers may not have access to data and thus cannot calculate ϕ with fitted propensity scores. Nevertheless, we provide a computation method for interested readers. This method is more robust than directly estimating the density and can be useful for simulation studies.

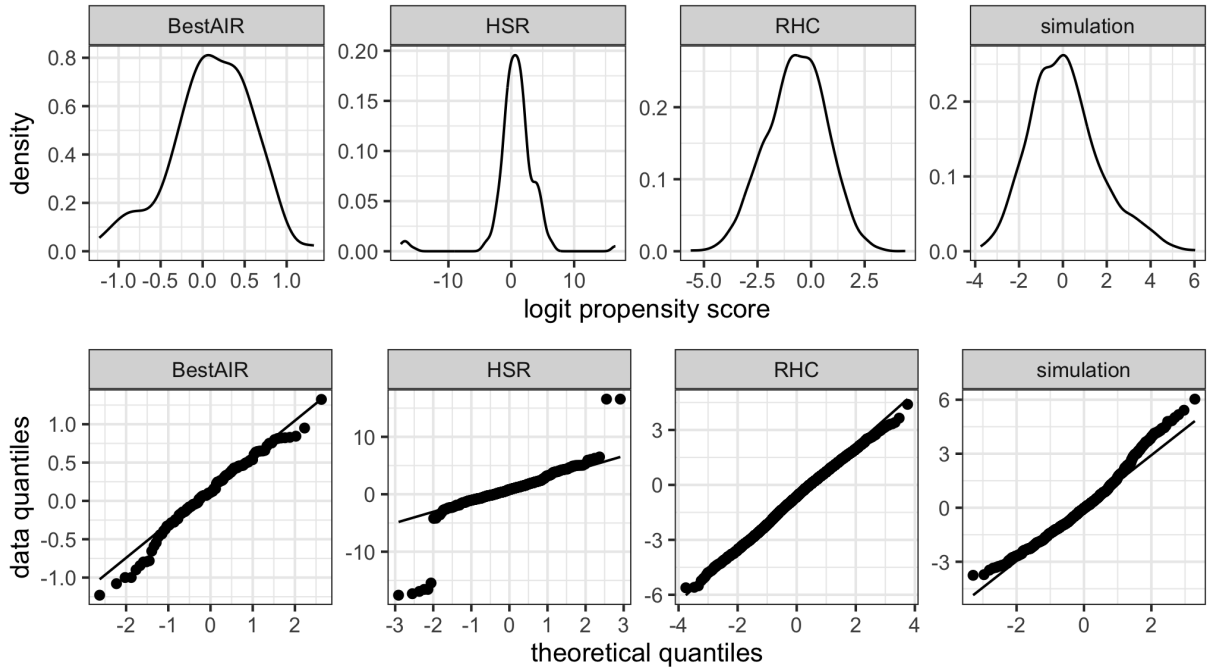


Figure 5: Density and Q-Q plots of the fitted logit propensity scores, a linear combination of covariates. The proximity of points to the reference line in the Q-Q plot shows the closeness of the distribution to a normal distribution.

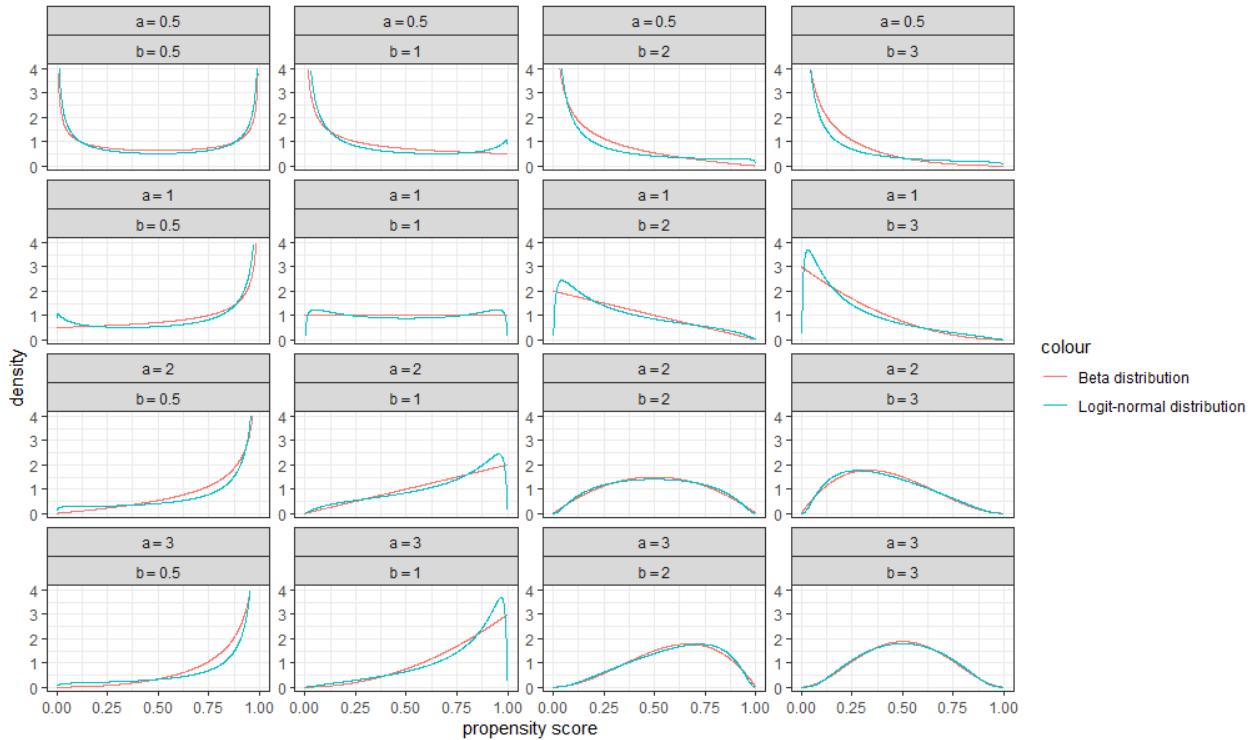


Figure 6: Examples of the Beta approximation to logit-normal distribution

Table 3: Sample size calculation by the proposed method, the two-sample z -test and the method in (Shook-Sa and Hudgens, 2022) to achieve nominal power of 0.80 under various degrees of overlap. The power is obtained from random sampling of the calculated size from the $N = 1,000,000$ units. The Monte Carlo error for a power of 0.8 is 0.004. The treatment proportion r is fixed at 0.5.

ϕ	ρ^2	R^2	Proposed			z -test			Shook-sa & Hudgens		
			Size	True PS	Est PS	Size	True PS	Est PS	Size	True PS	Est PS
1.00	0.00	0.13	992	0.81	0.85	977	0.80	0.83	977	0.80	0.83
0.98	0.02	0.13	1019	0.80	0.85	977	0.80	0.82	1016	0.80	0.85
0.93	0.02	0.12	1166	0.80	0.85	975	0.74	0.78	1157	0.80	0.85
0.88	0.01	0.12	1528	0.83	0.85	973	0.62	0.68	1489	0.80	0.85
0.84	0.01	0.12	1972	0.83	0.87	972	0.56	0.59	1914	0.82	0.86
0.81	0.01	0.12	2460	0.86	0.89	972	0.49	0.51	2342	0.83	0.87

By Bayes' theorem,

$$f_z(u) = \Pr(e(X) = u \mid Z = z) = \frac{\Pr(Z = z \mid e(X) = u) \Pr(e(X) = u)}{\Pr(Z = z)}. \quad (76)$$

Hence,

$$\phi = \int_0^1 \sqrt{f_0(u)f_1(u)} du = \frac{\int_0^1 \sqrt{u(1-u)} \Pr(e(X) = u) du}{\sqrt{r(1-r)}}. \quad (77)$$

Let $F(u) = \Pr(e(X) \leq u)$ be the CDF of $e(X)$. Let $\hat{e}_1, \hat{e}_2, \dots, \hat{e}_n$ be the estimated propensity scores of the units, and let $\hat{F}(u) = \frac{1}{n} \sum_{i=1}^n \mathbb{I}(\hat{e}_i \leq u)$ be the empirical CDF of $e(X)$. Then,

$$\phi = \frac{\int_0^1 \sqrt{u(1-u)} dF(u)}{\sqrt{r(1-r)}} \approx \frac{\int_0^1 \sqrt{u(1-u)} d\hat{F}(u)}{\sqrt{r(1-r)}} = \frac{1}{n} \cdot \frac{\sum_{i=1}^n \sqrt{\hat{e}_i(1-\hat{e}_i)}}{\sqrt{r(1-r)}}. \quad (78)$$

C Additional Simulation Results

C.1 Simulations with binary outcomes

We repeat the simulation design in Section 5.1, and dichotomize the potential outcome $Y_i(z)$ into a binary variable $Y_i^b(z) = \mathbb{I}(Y_i(z) > -2)$. The observed outcome $Y_i^b = Z_i Y_i^b(1) + (1 - Z_i) Y_i^b(0)$. The true ATE on Y^b is $\tau^b = \mathbb{E}[Y_i^b(1) - Y_i^b(0)] = 0.089$. Assume that we estimate τ^b using the Hájek estimator with Y_i^b . Dichotomizing $Y_i(z)$ does not affect the propensity scores, and hence ϕ remain unchanged from Simulation 5.1, while ρ^2, R^2 changed. The pooled $S^2 = r(1-r) = 0.25$. We inversely solve the sample size to reach a nominal power of 0.80, and show the results in Table 3.

From Table 3, the proposed method yields sample sizes achieving powers near 0.80, performing similarly to Shook-Sa and Hudgens (2022). In contrast, the two-sample z -test continuously leads to vastly underestimated sample size as the degree of overlap decreases.

C.2 Synthetic simulations with ATT and ATO estimands

With the same simulation design and data generating process as in Section 5.1, we focus on the ATT and ATO estimands, the true value of which are both 1. For $\kappa \in \{0, 0.25, 0.5, 0.75, 0.9, 1\}$, corresponding to $\phi \in \{1.00, 0.98, 0.93, 0.87, 0.84, 0.81\}$, we calculate the sample size of the Hájek estimator (16) for the ATT and ATO, with estimated and true propensity scores, respectively. Then we inverse the process under each scenario to calculate the power of the Hájek estimators; the results are shown in Table 4. In all scenarios, the estimated sample size is close to the true value 1000. As predicted from the general theory on the WATE (Li et al., 2018a), the ATT estimator has large variance than the ATO estimator. Consequently, given the same setting, the ATT requires larger sample size to achieve the same level of power the ATO, and the discrepancy increases as the degree of overlap decreases.

Table 4: Sample size (size) calculated by the proposed method to achieve the nominal power 0.8 under various degrees of overlap. The power is obtained from bootstrapping 10,000 random samples of the calculated size.

ϕ	ATT	Power		ATO	Power	
	Size	True PS	Est PS	Size	True PS	Est PS
1.00	629	0.86	0.80	629	0.87	0.80
0.98	661	0.88	0.80	653	0.85	0.79
0.93	772	0.86	0.80	697	0.80	0.76
0.88	1077	0.85	0.80	739	0.75	0.76
0.84	1457	0.84	0.79	774	0.76	0.78
0.81	1900	0.82	0.79	778	0.78	0.81

The sample sizes for ATT and ATO calculated with estimated propensity scores are not guaranteed to be conservative. However, this simulation shows that (i) the sample sizes calculated with the true and estimated propensity scores are similar, and (ii) the sample size for the ATO appears to be conservative if one uses the estimated propensity score in the study.

C.3 Synthetic simulations with heterogeneous treatment effect and ATT and ATO estimand

Table 5 extends the HTE simulation to the ATT and ATO estimands, using the true estimand-specific effect size $\tilde{\tau} = \tau^h/S$. The ATO remains well-calibrated, with empirical power near or above the nominal 0.80, consistent with its known efficiency and stability. The ATT, however, exhibits substantial power loss as overlap worsens – a sharp departure from the homogeneous case in Table 4.

As noted in Appendix C.2, the sample size for the ATT is not guaranteed to be conservative; under HTE, this issue is amplified. Since HTE inflates $\mathbb{V}\{Y(1)\}$ while leaving $\mathbb{V}\{Y(0)\}$ unchanged, and all observed outcomes in the ATT’s target population are $Y_i(1)$, the variance underestimation from the omitted $\mathbb{V}\{\tau(X)\}$ term (Remark 1) is particularly consequential for the ATT. Practitioners targeting the ATT should exercise greater caution when effect heterogeneity is suspected.

C.4 RHC simulation with ATT and ATO estimands

The Hájek estimate of the ATT is 0.070 (standardized effect size 0.15). The sample size calculated to achieve power 0.8 is 2449. With a sample of 2449 units, the bootstrap estimate of the power with $B = 1,000$ replications is 0.695 (95% CI: 0.666 to 0.724). Unlike the ATE where we overestimate the sample size, our

Table 5: Sample size (size) calculated by the proposed method to achieve the nominal power 0.8 under various degrees of overlap and HTE. The power is obtained from bootstrapping 10,000 random samples of the calculated size.

ϕ	ATT		Power		ATO		Power	
	τ^h	Size	True PS	Est PS	τ^h	Size	True PS	Est PS
<i>covariates-driven HTE</i>								
1.00	1.00	667	0.81	0.89	1.00	665	0.80	0.89
0.98	1.03	652	0.78	0.85	1.00	689	0.80	0.89
0.93	1.06	729	0.72	0.77	0.99	742	0.81	0.87
0.87	1.08	986	0.64	0.68	0.99	798	0.78	0.87
0.83	1.09	1317	0.56	0.59	0.99	828	0.77	0.85
0.81	1.09	1689	0.50	0.51	0.99	846	0.76	0.84
<i>propensity score-driven HTE</i>								
0.98	1.19	457	0.77	0.82	0.99	653	0.80	0.87
0.93	1.34	418	0.70	0.72	0.97	726	0.80	0.86
0.87	1.45	492	0.61	0.64	0.95	802	0.78	0.84
0.83	1.50	617	0.59	0.57	0.95	840	0.76	0.83
0.81	1.53	764	0.52	0.54	0.94	863	0.75	0.81

estimate for the ATT sample size is not guaranteed conservative. The Hájek estimate of the ATO is 0.075 (standardized effect size 0.16). The sample size calculated to achieve power 0.8 is 1546. With a sample of 1546 units, the bootstrap estimate of the power with $B = 1,000$ replications is 0.816 (95% CI: 0.792 to 0.840).